Modeling-Based Minimization of Time-to-Uniformity in Microwave Heating Systems

by

Brian G. Cordes

A Thesis

Submitted to the Faculty

of the

WORCESTER POLYTECHNIC INSTITUTE

in partial fulfillment of the requirements for the

Degree of Master of Science

in

Applied Mathematics

by

_____

May 2007

APPROVED:

_____

Dr. Vadim V. Yakovlev, Thesis Advisor

_____

Dr. Bogdan Vernescu, Department Head

Abstract

A fundamental problem of microwave (MW) thermal processing of materials is the intrinsic non-uniformity of the resulting internal heating pattern. This project proposes a general technique to solve this problem by using comprehensive numerical modeling to determine the optimal process guaranteeing uniformity. The distinctive features of the approach are the use of an original concept of uniformity for MW-induced temperature fields and pulsed MW energy as a mechanism for achieving uniformity of heating.

The mathematical model used to represent MW heating describes two component physical processes: electromagnetic wave propagation and heat diffusion. A numerical solution for the corresponding boundary value problem is obtained using an appropriate iterative framework in which each sub-problem is solved independently by applying the 3D FDTD method. Given a specific MW heating system and load configuration, the optimization problem is to find the experiment which minimizes the time required to raise the minimum temperature of the load to a prescribed goal temperature while maintaining the maximum temperature below a prescribed threshold. The characteristics of the system which most dramatically influence the internal heating pattern, when changed, are identified through extensive modeling, and are subsequently chosen as the design variables in the related optimization. Pulsing MW power is also incorporated into the optimization to allow heat diffusion to affect cold spots not addressed by the heating controlled by the design variables.

The developed optimization algorithm proceeds at each time-step by choosing the values of design variables which produce the most uniform heating pattern. Uniformity is measured as the average squared temperature deviation corresponding to all distinct neighboring pairs of FDTD cells representing the load. The algorithm is implemented as a collection of *MATLAB* scripts producing a description of the optimal MW heating process along with the final 3D temperature field.

We demonstrate that CAD of a practical applicator providing uniform heating is reduced to the determination of suitable design variables and their incorporation into the optimization process. Although uniformity cannot be attained using “static” MW heating, it is achievable by applying an appropriate pulsing regime. The functionality of the proposed optimization is illustrated by computational experiments which show that time-to-uniformity can be reduced, compared to the pulsing regime, by up to an order of magnitude.

This Master’s Thesis project was sponsored by The Ferrite Company, Inc., Nashua, NH.

Acknowledgments

- Vadim Yakovlev for being an exceptionally patient and dedicated advisor.
- The Ferrite Company, Inc. for sponsoring this research.
- Gene Eves, Tom Wendel, and Bruce Secovich of The Ferrite Company, Inc. for their help in making this entire project a success.
- *QWED* for providing a special temporary license for *QuickWave-3D*.
- Mom, Dad, and Andrew for everything in between that matters most.

Table of Contents

List of Figures

List of Tables

Chapter 1

Introduction

It is widely known that microwave (MW) heating can improve the efficiency and quality of a variety of applied thermal processes, like food processing, sterilization, pasteurization, drying of wood, vulcanization of rubber, waste processing and recycling, mineral processing, etc. [Metaxas and Meredith, 1983; Thuery, 1992; Microwave Processing, 1994; Roussy and Pearce, 2001; Ohlsson, et al, 2006]. Recent discoveries have also demonstrated the potential for using microwave energy as a supplemental tool in a wide array of new areas of science and engineering – from enhanced/accelerated organic synthesis reactions and medical therapy [Whittaker and Mingus, 1994; Kappe and Stadler, 2005; Lidström and Tierney, 2005; Loupy, 2006] to production of novel materials with unique characteristics via sintering metal powder and nano-composites [Agrawal, 1999; Bykov, et, al, 2001; Leparoux, et al, 2003; Feher, et al, 2006; Petzold, et al, 2006].

Despite these new advances, the MW power industry still suffers from the same fundamental problem that has remained unsolved ever since the emergence of the field, specifically, the intrinsic non-uniformity of MW-induced internal heating patterns. Experimental evidence of this fact can be found in literature (see, e.g., [Bradshaw, et al, 1997; Nott, et al, 1999; Araszkiewicz, et al, 2007]). Examples of surface and internal heating patterns measured using infrared and magnetic resonance imaging techniques are shown in Figs. 1.1 and 1.2, respectively. Since most applications require uniformity of heating and the success of these applications depends substantially on the ability to efficiently control the resulting heating

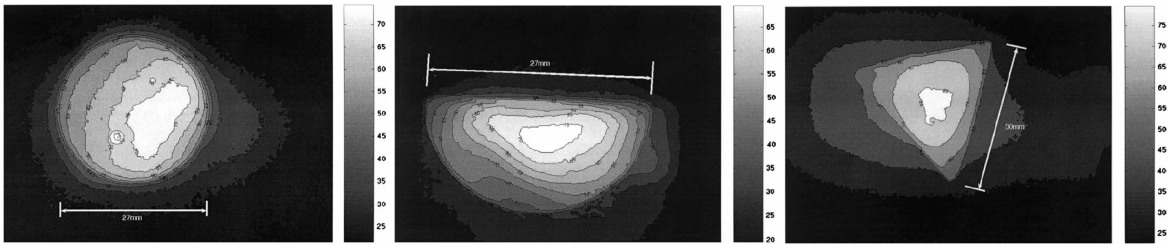

(a) (b) (c)

Fig. 1.1. Infrared images of MW-induced heating patterns in moisturized gypsum of spherical (a), half-cylindrical (b) and prismatic (triangle base) configuration (c) [Araszkiewicz, et al, 2007]

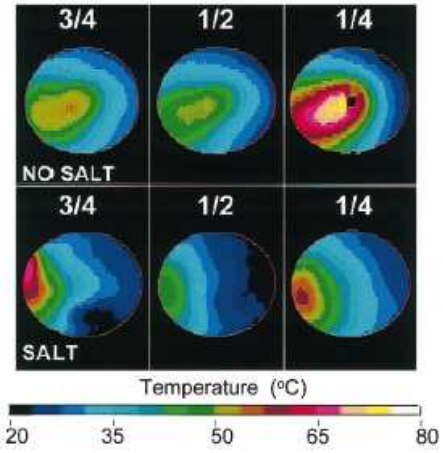

Fig. 1.2. Magnetic resonance images of MW-induced heating patterns for TX151 gel in a cylindrical jar [Nott, et al, 1999].

process, the recent discoveries for new uses of MW energy have dramatically increased the importance of developing general techniques for creating practical systems which ensures uniformity (see, e.g., [Metaxas and Meredith, 1983; Buffler, 1993; Chan and Reader, 2000; Zhang and Datta, 2000; Egorov, et al, 2006].) However, because of exceptional complexity of the physics of the process, internal/volumetric character of heat release making it difficult to experimentally study the phenomenon, variation of essential material parameters with temperature and other reasons, very little has been done so far towards obtaining a general

solution of this fundamental problem. Below we briefly review the current state-of-the-art research in the related field.

The traditional approach for improving MW heating systems has been experimentation. An analysis of results published on this topic indicates that there is no commonly accepted technique for measuring uniformity and no standard formulation for the corresponding optimization problem. For instance, while some researchers believe that the temperature field can be homogenized by evening up the pattern of the electric field [Kolomeytsev and Yakovlev, 1993; Bernhard and Joines, 1996; Sundberg, et al, 1998; Lurie and Yakovlev, 1999 & 2002; Pitarch, et al, 2003; Plaza-Gonzalez, et al, 2004, 2005; Balbastre, et al, 2006; Dominguez-Tortajada, et al, 2007; Pedreño-Molina, et al, 2007; Komarov and Yakovlev, 2007], other authors quantify the level of uniformity of MW heating through the spatial distribution of dissipated power [Bradshaw, et al, 1997 & 2003; Wäppling-Raaholt, et al, 2006].

Given the continually expanding capabilities of computer hardware, an alternative approach to direct experimentation that has recently gained certain popularity is computer modeling [Hill and Marchant, 1996; Risman and Celuch, 2000; Yakovlev, 2001 & 2006; Gwarek and Celuch, 2006 & 2007]. Moreover, the increasing demand for general purpose multi-physical modeling software has resulted in the development of several advanced modeling tools. In particular, a number of commercial products currently exist which are capable of effectively modeling the electromagnetic component of MW heating [Yakovlev, 2006].

The interaction of high frequency electromagnetic waves with materials is a complex multiphysics phenomenon, and two specific component processes must be considered, at the least, to define a relatively accurate representative mathematical model. Specifically, these are electromagnetic wave propagation and heat diffusion which can be independently modeled using Maxwell's equations and the heat transfer equation, respectively. Other physical phenomena may also be present in MW heating processes (e.g. phase change, mass and fluid transport, evaporation, etc., see, e.g., [Jumah and Raghavan, 2004; Salagnac, et al, 2004]), but can be considered of secondary nature in terms of their importance in solving the problem of uniformity.

Numerical solutions for multiphysics problems can be obtained by applying either weak coupling or strong coupling algorithms. Strong coupling algorithms solve all governing equations simultaneously using a

single time-step. For the problem of MW heating, this technique would be both unfeasible and inefficient due to the complexity of practical systems and the dramatic difference between the time-scales of the electromagnetic (EM) and thermal (T) processes. Rather, the most efficient computational option is to apply a weak coupling algorithm in which each sub-problem is solved individually applying different time-steps.

When material parameters are temperature-independent, weak coupling can be implemented by solving the electromagnetic problem once and using the computed electric field as a source in the thermal model. The output of the latter is the resulting temperature field of the processed material. Such an approach has been exercised in a number of publications dealing with the modeling of practical systems, e.g., in [Datta and Hu, 1992; Lagos, et al, 1995; Balat-Pichelin and Duqueroie, 2001; Gjonaj, et al, 2002; Badics, et al, 2004; Huo and Li, 2005; Sabliov, et al, 2005; Knoerzer, et al, 2006; Wappling-Raaholt, et al, 2006; Wappling-Raaholt and Ohlsson, 2006; Sabliov, et al, 2007].

When material parameters are temperature-dependent, weak coupling can be implemented by partitioning the total heating time into a set of time-steps in which the electromagnetic portion of the problem is solved using the current material parameters, the thermal portion is solved over the current time-step using the computed solution of the electric field, followed by the update of material parameters based on the new temperature field. Examples of this approach can be found in the studies by Jolly and Turner [1990], Choi and Konrad [1991], Sekkak, et al [1994], Ma, et al [1995], Clemens and Saltiel [1996], Craven, et al [1996], Torres and Jecko [1997], Alpert and Jerby [1999], Conner, et al [1999], Heidemann, et al [2000], Lu, et al [2000], Michalski and Jabs [2000], Zhao and Turner [2000], Pichon and Meyer [2002], Ratanadecho, et al [2002a & 2002b], Kopyt and Celuch [2003, 2005a & 2007], Rabello, et al [2005], and Zhu, et al [2007]. The above studies consider systems ranging from one dimension [Jolly and Turner, 1990; Alpert and Jerby, 1999; Michalski and Jabs, 2000], to two dimensions [Choi and Konrad, 1991; Clemens and Saltiel, 1996; Craven, et al, 1996; Conner, et al, 1999; Pichon and Meyer, 2002; Ratanadecho, et al, 2002a; Ratanadecho, et al, 2002b], to three dimensions [Sekkak, et al, 1994; Ma, et al, 1995; Torres and Jecko, 1997; Heidemann, et al, 2000; Lu, et al, 2000; Zhao and Turner, 2000; Kopyt and Celuch, 2003, 2005a, 2007; Rabello, et al, 2005; Zhu, et al, 2007].

The majority of explorations which attempt to solve the coupled EM-T problem consider using either the finite-element method (FEM) or the finite-difference time-domain method (FDTD). The general opinion during 1980-1990s was that FEM was the most powerful tool available. However, recent studies have identified 3D conformal FDTD techniques as the most efficient and accurate numerical schemes for EM modeling of systems and processes of MW heating [Yakovlev, 2006]. For most adequate modeling of temperature fields, these algorithms should be coupled with an efficient technique that performs thermal analysis, for instance, with either FDTD- [Celuch, et al, 2006; Tilford, et al, 2007] or FEM-based solution methods [Kopyt and Celuch, 2005a,b].

Several experimental techniques potentially capable of making the temperature field more uniform have been modeled; those include rotation of the load [Kopyt and Celuch, 2003], mode stirrers [Plaza-Gonzalez, et al, 2004, 2005], multiple feeds [Pitarch, et al, 2003], sample movement [Pedreño-Molina, et al, 2007], dielectric layers occupying a part of the cavity [Bernhard and Joines, 1996; Lurie and Yakovlev, 1999 & 2002], dielectric casts surrounding the load [Monzo-Cabrera, et al, 2007], and design of the load and/or its container [Wappling-Raaholt, et al, 2006]. Pulsing MW energy is also known to be a useful technique because it employs the natural mechanism of heat diffusion to improve the uniformity of the temperature pattern. Indeed, since the rate of MW heating is normally much higher than the rate of heat relaxation, it would be unreasonable to expect that heat diffusion could reduce the non-uniformity of the temperature field while MW power is applied to the system. However, this effect would be obviously possible if MW power is turned off. This leads us to the idea of a special regime which allows periods of thermal relaxation to occur between periods of MW heating.

The concept of pulsed MW heating has existed for a quite some time; the technique has been experimentally tested in drying of polyurethane foam [Jolly, 1986], grain [Gunasekaran, 1990], wood [Brelid and Simonson, 1999] as well as in food processing [Yongsawatdigul and Gunasekaran, 1996; Haugh, et al., 1997; Schaefer, 1999; Groombridge, et al., 2000; Yang and Gunasekaran, 2001; Knoerzer, 2006; Gunasekaran and Yang, 2007a & 2007b]. These works demonstrate that pulsing microwave treatment results in an overall more uniform temperature distribution than continuous processing. Known computational efforts, however, are limited to the study by Yang and Gunasekaran [2004] employing a simplistic Lambert's

law-based calculation of temperature in an axially symmetric scenario with a cylindrical sample of small diameter as well as the report by Feldman, et al [2007] which considers analytical-numerical 1D model and FEM-based 2D model. The benefits of applying MW pulsing are illustrated in their results, but more general computational studies are needed to find an appropriate balance between heating and relaxation periods. This provides direct motivation for considering MW pulsing as an assisting mechanism for achieving complete MW heating uniformity.

This Thesis proposes an efficient general technique for solving the problem of non-uniform MW heating by using comprehensive numerical modeling to simulate preliminary experiments and by synthesizing the optimal process guaranteeing uniformity. In the developed approach, we simulate the MW heating process by solving the EM and T components of the coupled problem using the 3D conformal FDTD method. Implementation of this technique is provided by the full-wave electromagnetic modeling software *QuickWave-3D*[1] with the associated *QW Basic Heating Module*. We introduce and provide corresponding implementations for the concepts of MW heating processes with variable characteristics and pulsing MW energy.

A formulation for the optimization problem is proposed which considers minimizing the time required to raise the minimum temperature of the material to a prescribed goal temperature while maintaining the maximum temperature below a prescribed threshold. Design variables in the related optimization are chosen to be the characteristics of the given MW system which produce the most dramatic affect on the heating pattern when changed. A corresponding optimization algorithm is developed that operates by choosing the values of design variables which produce the most uniform heating pattern at each time-step. Uniformity of the heating pattern is measured as the average squared temperature deviation corresponding to all distinct neighboring pairs of FDTD cells which determine the load in the resulting discretization of the problem.

The developed analysis and optimization algorithms are implemented as two distinct pieces of software written using *MATLAB*[2]. Simulations are managed within the *MATLAB* environment by calling *QW-*

[1] *QuickWave-3D*™, QWED Sp. z o. o., ul. Piêkna 64A m 11, 00-672 Warsaw, Poland, http://www.qwed.com.pl/.

[2] *MATLAB*™, The MathWorks, Inc., 3 Apple Hill Drive, Natick, MA 01760-2098 http://www.mathworks.com/.

Editor and *QW-Simulator*, the two main components of *QuickWave-3D*, from the command line when necessary.

We demonstrate that computer-aided design (CAD) of a practical applicator providing uniform heating is reduced to the determination of suitable design variables and their incorporation into the optimization process. We show that although uniformity cannot be achieved using "static" MW heating, it is possible to reach a desired level of uniformity by applying an appropriate pulsing regime. However, the time required for this is much too large to be considered for practical application. We provide the details of several computational experiments that were performed which illustrate that by applying the proposed optimization technique, the time-to-uniformity can be reduced by up to an order of magnitude when compared to applying a pulsing regime alone.

Chapter 2

Modeling Microwave Heating

The results presented in this Thesis are entirely based on data that is obtained by solving a mathematical model which describes the physical process of MW heating. We focus our efforts on developing suitable numerical techniques as opposed to direct experimentation because of the generality of the problem we are trying to solve.

2.1 Mathematical Description of the Physical Problem

The two physical processes that can form an appropriate basis for the process of MW heating are electromagnetic wave propagation and heat diffusion. Other physical phenomena involved, e.g., mass and fluid transport and evaporation, are not considered in our model because of their lack of influence on the uniformity of heating. Moreover, incorporating these additional phenomena into our model would enormously increase the complexity of the analysis whereas the major objective of this study is the development of original optimization concepts and techniques.

Electromagnetic wave propagation is described mathematically by Maxwell's equations:

$$\nabla \cdot \varepsilon'(T)\varepsilon_0 \mathbf{E} = \rho \tag{1}$$

$$\nabla \times \mathbf{E} = -\mu_0 \frac{\partial(\mu \mathbf{H})}{\partial t} \tag{2}$$

$$\nabla \times \mathbf{H} = \sigma(T)\mathbf{E} + \varepsilon_0 \frac{\partial(\varepsilon'(T)\mathbf{E})}{\partial t} \tag{3}$$

$$\nabla \cdot \mu\mu_0 \mathbf{H} = 0 \tag{4}$$

where **E** is the electric field intensity, **H** is the magnetic field intensity, ρ is the charge density, σ is electrical conductivity, ε_0 is the permittivity of free space, ε' is permittivity (dielectric constant), μ_0 is the permeability of free space, and μ is permeability. Heat diffusion is described mathematically by the heat transfer equation

$$\delta(T)c(T)\frac{\partial T}{\partial t} - \nabla \cdot (k(T)\nabla T) = Q_{\text{source}} \tag{5}$$

where T is temperature, δ is density, c is specific heat, k is thermal conductivity and Q_{source} is the heat source. In this model, it is assumed that the electric and thermal material parameters ε, σ, δ, c, and k are temperature dependent.

Combining equations (1-5) and appropriate boundary conditions, we can mathematically describe the MW heating process in time and space as the following boundary value problem:

$$\nabla \times (\mu^{-1}\nabla \times \mathbf{E}) = \left(\frac{\omega}{c}\right)^2 \left(\varepsilon'(T) - i\frac{\sigma(T)}{\omega\varepsilon_0}\right)\mathbf{E}, \tag{6}$$

$$\rho(T)c(T)\frac{\partial T}{\partial t} - \nabla \cdot (k(T)\nabla T) = \sigma(T)\left|\mathbf{E}\right|_{\text{avg}}^2 = \omega\varepsilon_0\varepsilon''(T)\left|\mathbf{E}\right|_{\text{avg}}^2, \tag{7}$$

$$\mathbf{E} \times \mathbf{n} = 0, \quad (\mathbf{E}_1 - \mathbf{E}_2) \times \mathbf{n} = 0, \tag{8-9}$$

$$T\Big|_{\Omega_A} = T_S, \quad \left.\frac{dT}{d\mathbf{n}}\right|_{\Omega_B} = 0, \tag{10-11}$$

where $\Omega = \Omega_A \cup \Omega_B$ represents the surface of the heated object and $\Omega_A \cap \Omega_B = \emptyset$.

2.2 Solution Algorithm for the Coupled Problem

Due to the presence of complex boundary conditions, the generalized problem has no analytical solution. The solution of the problem can only be approximated with the use of numerical methods. Since we consider the electric material parameters to be temperature dependent, the mathematical equations are coupled and we must investigate the physics of the modeled process in order to develop an effective solution technique.

From a physical perspective, the most noticeable feature of MW heating is the dramatic difference between the time-scales at which the EM and T processes operate, specifically nanoseconds and real time (seconds). The proposed efficient solution algorithm addresses this characteristic by solving each sub-problem independently using a specific iterative framework by partitioning the total heating time into a series of time-steps.

In each time-step, the electromagnetic problem is solved first using the current material parameters. The thermal portion of the problem is then solved using the computed electric field as the source in the thermal model, and material parameters are updated based on the new temperature field. The size of each heating time-step depends on how quickly electric material parameters change as a function of temperature. An illustration of this process is shown in Fig. 2.1.

The most common numerical methods used to solve electromagnetic problems are the finite-element method (FEM) and the finite-difference time-domain (FDTD) method. Each technique can be considered more appropriate for solving particular classes of such problems, but FEM is more difficult to implement and also has significantly higher memory requirements [Swanson and Hoefer, 2003]. Specifically, for high-frequency EM problems, the 3D conformal FDTD technique is generally faster than FEM and also allows for simulating electrically large systems which may be unfeasible for the FEM-based algorithms [Gwarek and Celuch, 2007].

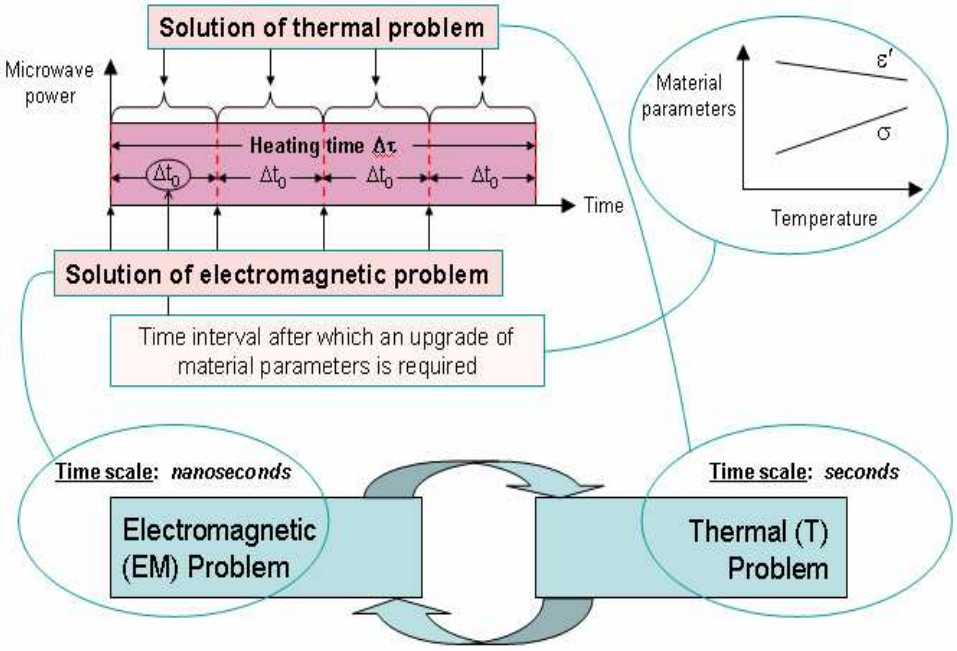

Fig. 2.1. Concept of efficient numerical solution of the EM-T coupled problem.

In solving the EM problem, the finite-difference time-domain (FDTD) method uses the central difference formula to approximate the spatial and temporal derivates in Maxwell's equations to obtain an explicit finite-difference approximation:

$$\frac{\partial F^n(i,j,k)}{\partial x} \approx \frac{F^n(i+1/2,j,k) - F^n(i-1/2,j,k)}{\delta} \tag{12}$$

$$\frac{\partial F^n(i,j,k)}{\partial t} \approx \frac{F^{n+1/2}(i,j,k) - F^{n-1/2}(i,j,k)}{\Delta t} \tag{13}$$

where $F = F(x,y,z,t)$ is a function of space and time, $\delta = \min\{\Delta x, \Delta y, \Delta z\}$ is the space increment, Δt is the time increment, and $F^n(i,j,k) \equiv F(i\delta, j\delta, k\delta, n\Delta t)$. The field components are interlaced within the unit cell and are evaluated at alternate half-time steps (Fig. 2.2) to obtain the system of scalar equations describing the

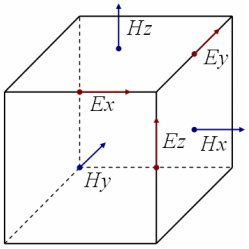

Fig. 2.2. Layout of the electric and magnetic field components in a 3D FDTD cell.

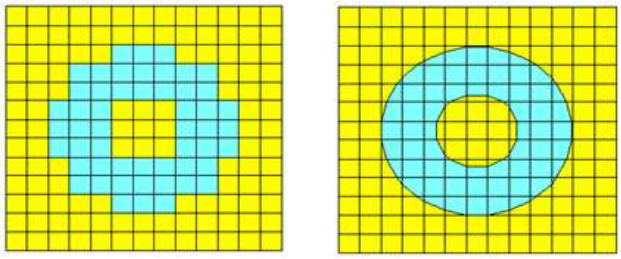

(a) (b)

Fig. 2.3. Discretization of a coaxial line with classical stair-case (a) and conformal FDTD meshes (b).

field components. To ensure accuracy of the method, δ must be small in comparison with the wavelength, and to ensure stability Δt must satisfy the Courant stability criterion:

$$\Delta t \leq \frac{\delta}{c\sqrt{3}} \tag{14}$$

The recently developed conformal FDTD method is significantly more powerful than classical FDTD because it allows each mesh cell to contain more than one media [Swanson and Hoefer, 2003; Gwarek and Celuch, 2007]. With this feature, the conformal FDTD method is capable of accurately describing complex geometries using reasonable meshes. This is impossible in the case of classical FDTD since an accurate description would most likely require a significant reduction in cell-size to mitigate the effects of the so called “stair-case” mesh, as demonstrated in Fig. 2.3.

Numerical results for the EM and T portions of the problem are obtained using the full-wave 3D conformal FDTD simulator *QuickWave-3D* (*QW-3D*) and the *QW Basic Heating Module* (*QW-BHM*), respectively. Fig. 2.4 described the implementation of the FDTD-based solution of the EM-T coupled problem. After reaching the FDTD steady-state for the EM solution, *QW-BHM* is invoked and proceeds by calculating average dissipated power and updating temperature. The *QW Heat Flow Module* (*QW-HFM*), which is responsible for solving the T portion of the problem, is then called and returns the diffused enthalpy field. *QW-BHM* finishes by updating temperature based on the diffused enthalpy field, and by updating material parameters based on the new temperature field. This process repeats until the desired total heating time has been reached.

2.3 Heating with Pulsing Microwave Energy

The goal of this research is to develop a technique which will allow us to have improved control over the heating pattern so that we are able to maintain and optimize uniformity of MW thermal processing. However, it is essentially impossible to obtain uniformity using MW heating alone due to the formation of stable hot and cold spots. Since our control over the heating pattern will thus gradually diminish as these hot and cold spots evolve over time, we are prompted to search for a reliable regime that can counteract this evolution process.

We consider using the natural mechanism of heat diffusion to improve the uniformity of the temperature field since it effectively relaxes hot and cold spots. However, the rate of energy absorption due to MW heating is much higher than the rate of energy release due to heat diffusion which is an indication that this process will most likely be unable to improve the uniformity of the temperature field while MW power is applied to the system. We thus introduce the idea of a pulsing regime where MW energy is turned off to allow for periods of relaxation between periods of heating.

In the developed algorithm, the total heating time is partitioned into a series of time-steps. Then, each time-step is partitioned into two sub-time-steps in which microwave heating is simulated in the first

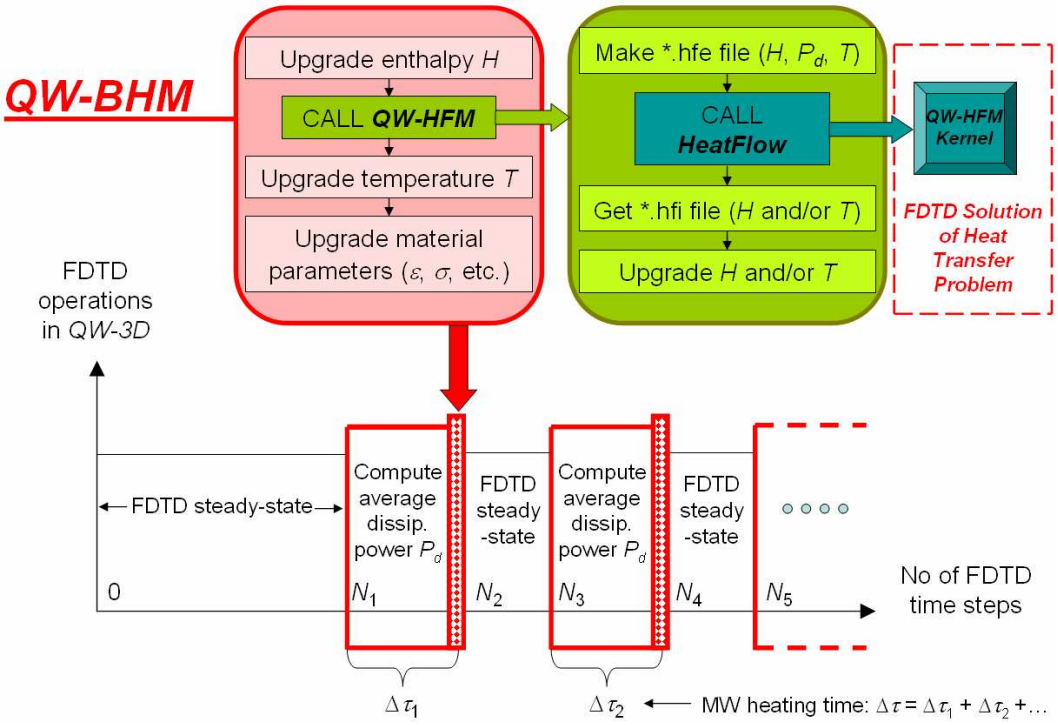

Fig. 2.4. FDTD solution of the EM-T coupled problem with the 3D conformal FDTD method using a combination of *QW-3D* and *QW-BHM*.

sub-time-step, but only thermal relaxation is simulated in the second sub-time-step. This is accomplished in the usual fashion by first solving the electromagnetic portion of the problem using the current material parameters and by solving the thermal portion using the computed electric field as the source in the thermal model. However, the thermal portion is solved over the entire heating time-step, whereas the source term in the thermal equation only accounts for application of MW power during the first sub-time-step. After the thermal problem is solved, material parameters are then updated based on the new temperature field. In this algorithm, the size of each time-step is determined by the size of each sub-time-step, where the first sub-time-step depends on how quickly electrical material parameters change as a function of temperature and the second sub-time-step depends on how much time is needed for relaxation.

Based on the described solution algorithm, pulsing has been incorporated into the *QW-3D* / *QW-BHM* implementation of the coupled EM-T solution algorithm by altering the *QW-BHM* mode of operation,

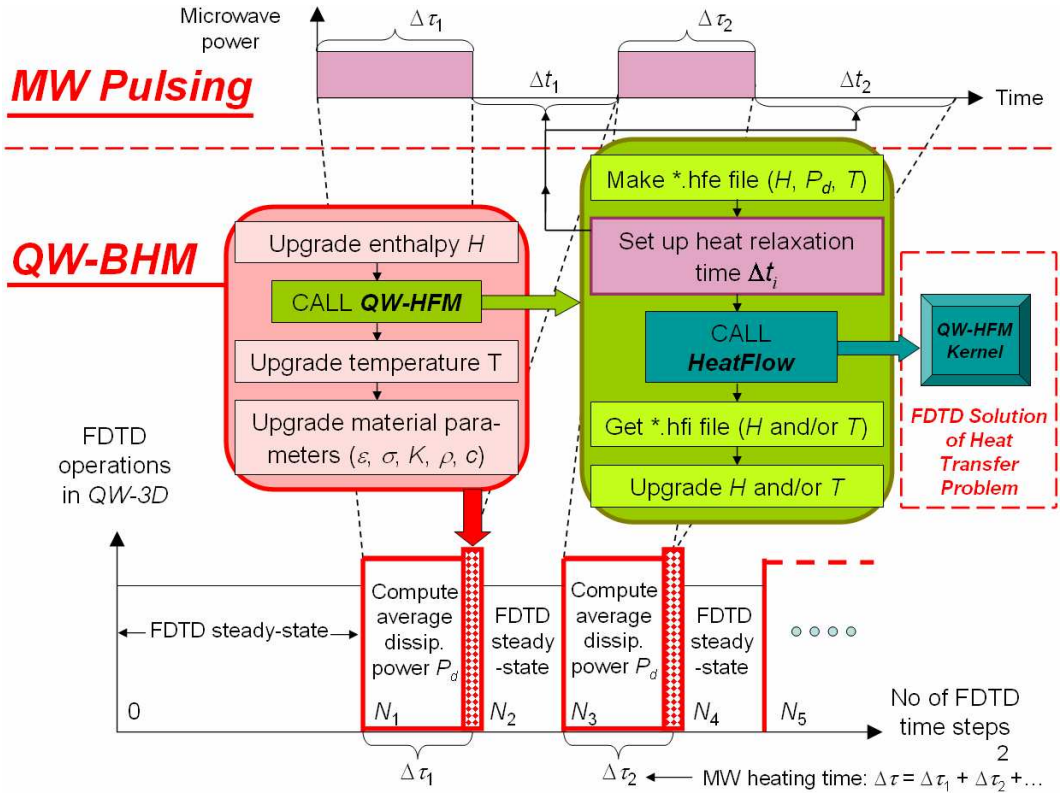

Fig. 2.5. Implementation of MW pulsing within the combined operation of *QW-3D* and *QW-BHM*.

as shown in Fig. 2.5. Instead of calling `hfm.exe` within the *QW-HFM* module, a batch file is used to control the heat flow process. Specifically, after reaching the FDTD steady-state for the EM solution, *QW-BHM* is invoked and proceeds by calculating average dissipated power and by updating temperature. After *QW-HFM* is called and the corresponding `*.hfe` file is created, the batch file changes the relaxation time specified within the `*.hfe` file to the appropriate value. The T problem is then solved by calling `hfm.exe` which returns the diffused enthalpy field. *QW-BHM* finishes by updating temperature based on the diffused enthalpy field, and by updating material parameters based on the new temperature field. This process repeats until the desired total heating time has been reached.

2.4 Heating with Variable Characteristics of the Process

Since this project is focused on performing optimization of a MW heating process, we must consider which general parameters should be used as design variables. More specifically, since our aim is to improve heating uniformity, we determine how we can alter the resulting heating pattern to improve uniformity. It is known from experimentation and modeling that significant changes in the heating pattern can be obtained by modifying the design parameters of MW systems. We thus introduce the concept of MW heating with variable characteristics and subsequently use this idea as a source for formulating a suitable optimization problem and corresponding algorithm.

Given that the optimization procedure will be based in part on this concept, we should be able to accurately and efficiently simulate complex MW scenarios in which design parameters change over the course of time. However, the parameters of interest (ones that determine the MW system) cannot be changed during the normal operation of the *QW-3D* software. Hence, we develop a corresponding implementation for this concept.

From the analysis of the structure and operation principles of *QW-BHM*, we are able to simulate complex MW heating experiments by managing the `*.hfi` file that is produced by the `hfm.exe` executable file which solves the T portion of the problem. We are able to reload the saved fields described within this `*.hfi` file back into the *QW-Simulator* core by further modifications of the developed batch file introduced in the previous section.

After initializing the simulation and making necessary changes to the model by calling *QW-Editor*, we choose our heating time and then simulate the model by calling *QW-Simulator*. This simulation is performed using the same algorithm described earlier which includes the option of specifying an additional relaxation time. After this simulation is finished, we save the resulting `*.hfi` file and determine the next set of values for the model parameters. If this new set of values is different from the previously used set, we make the necessary modifications to the model by calling *QW-Editor* and update the saved `*.hfi` file accounting for any changes in the meshing and position of the load. We then choose our next heating time

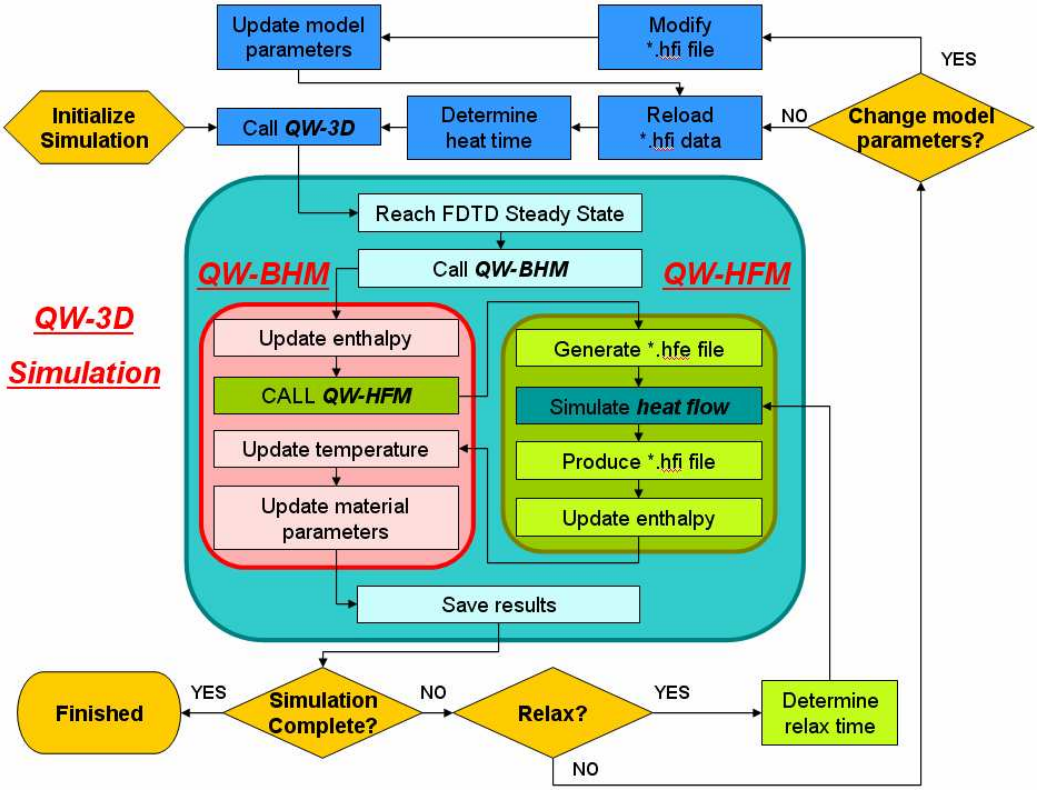

Fig. 2.6. Flow-chart for advanced simulation regime.

and perform the next simulation based on the data from the saved `*.hfi` file, which is reloaded back into *QW-Simulator*. This process repeats until the desired total heating time has been reached. A detailed flow-chart of the entire process is presented in Fig. 2.6.

The described algorithm is implemented as a collection of controlling scripts and post-processing functions written using *MATLAB*. Simulations are managed within the *MATLAB* environment by calling *QW-Editor* and *QW-Simulator* from the command line when necessary.

2.5 Innovations of the Developed Modeling Software

This section briefly summarizes the advances made in the present project in comparison with the earlier available computational opportunities. Based on the implementation of the coupled EM-T solution algorithm

provided by the combination of *QW-3D* and *QW-BHM*, we have developed general modeling software that is capable of simulating complex MW heating scenarios which can simultaneously incorporate the concepts of variable characteristics and pulsing MW energy.

Simulations are specified in terms of the modifications of model parameters and two possible formats for providing these modifications are offered. Modifications can be specified either directly, by providing pairs of model configurations and times which precisely determine when the model should be changed and what parameters should be changed, or indirectly, by providing pairs of model configurations and conditions which must be satisfied for the corresponding design to take effect.

The software is capable of modifying the value of any characteristic defined within the developed parameterized model of a MW system which is provided by the *QW-3D* `*.udo` file. The varying properties of the model which were tested include:

- the position of any modeled object,
- the dimensions of any modeled object,
- the exciting mode(s) for any feed in the system,
- the input power for any feed in the system,
- the phase shift between simultaneously active modes for any feed in the system.

This list can naturally be extended to include additional modeling features available in *QW-3D*.

The modification of design parameters is accomplished by altering the *QW-3D* `*.udo` file before the simulation is performed so that all properties of the model are read from a text file.

Chapter 3

Optimization of Microwave Heating

The first step towards developing a precise definition for the optimization problem is to formulate the overall objectives and constraints associated with a MW heating scenario to be analyzed in terms of uniformity.

3.1 Concept of Time-to-Uniformity

In practical applications, a material is said to be heated uniformly if the maximum and minimum temperatures of the heated material lie within an allowable interval (T_{MIN}, T_{MAX}). Based on this characterization, we define the goal of each MW heating experiment to be to raise the minimum temperature of the load, T_m, to a prescribed goal temperature, T_{MIN}, while maintaining the maximum temperature, T_M, below a prescribed threshold, T_{MAX}. The time required to achieve this goal temperature is denoted the time-to-uniformity, t_u. As explained in Chapter 2, each experiment will inevitably rely on the application of MW pulsing as an efficient supplement in reaching the desired level of uniformity. MW energy is turned off once T_M reaches T_{MAX} and resumes once T_M has relaxed below some lower bound, as illustrated in Fig. 3.1.

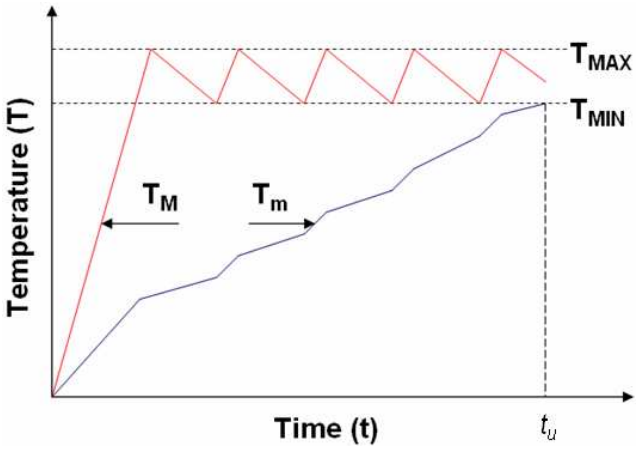

Fig. 3.1. Conventional time characteristic of the concept of time-to-uniformity: T_M, T_m are the maximum, minimum temperatures of the load; (T_{MIN}, T_{MAX}) is the required range for T_M and T_m to reach uniformity.

3.2 Homogenizing the Temperature Field – Optimization Problem

The unique step-by-step description of a given MW heating process in terms of the modification of model parameters as a function of time is defined as the corresponding *operating procedure*.

Using the proposed concepts of time-to-uniformity and operating procedure, we mathematically define the optimization problem as follows: given a specific MW heating system and load configuration, find the operating procedure $P^* \in \Omega$ which satisfies

$$t_u(P^*) = \min_{P \in \Omega} t_u(P), \tag{15}$$

where Ω is the set of all operating procedures P which satisfy

$$T_M(t, P) \le T_{MAX} \quad \text{for all } t > 0. \tag{16}$$

In this situation, an operating procedure reduces to the unique description of a MW heating process in terms of the time-specific modifications of chosen design variables. More importantly, the entire optimization problem can be alternatively formulated as the minimization of time-to-uniformity.

Specifically, in accordance with Section 2.4, we are interested in the parameters of the given MW heating system (e.g., cavity dimensions, load position, excitation settings, etc.) which most dramatically affect the temperature pattern when changed. Since the efficiency and performance of the optimization depend on the quality of the set of provided design variables, we must first conduct an extensive analysis testing possible combinations of values for design parameters to be able to identify the best possible choices. With the results of this analysis, we should be in a position to choose, in accordance with some particular related criterion and certain technological constraints and conditions, the design variables for the problem (15), (16).

Furthermore, this preliminary analysis is necessary because the actual heat released in the processed material essentially depends on the properties of the load, particularly on the loss factor and thermal conductivity [Pitarch, et al, 2003; Plaza-Gonzalea, et al, 2004; Balbastre, et al, 2006; Monzó-Cabrera, et al, 2007]. The solution of the uniformity problem depends substantially on the scenario, and general trends in the temperature distribution in the heated materials are hardly predictable.

The suggested technique is noticeably different from the methods which could be considered relevant: in the techniques of optimal control by Banga [Banga, et al, 2001, Balsa-Canto, et al, 2002; Banga, et al, 2003], the MW energy, as a source of heating, is not considered at all. In [Itaya, et al, 2007], the dynamic control over MW heating is implemented only through variable source power conditioned by online temperature measurement whereas the technique proposed in this project is based on data from preliminary simulations which includes testing all characteristics of the process that are accessible for modeling.

3.3 Optimization Algorithm

The optimization algorithm proceeds at each heating step by choosing, among all tested configurations, the set of values of design variables which produce the most uniform heating pattern. The temperature field that

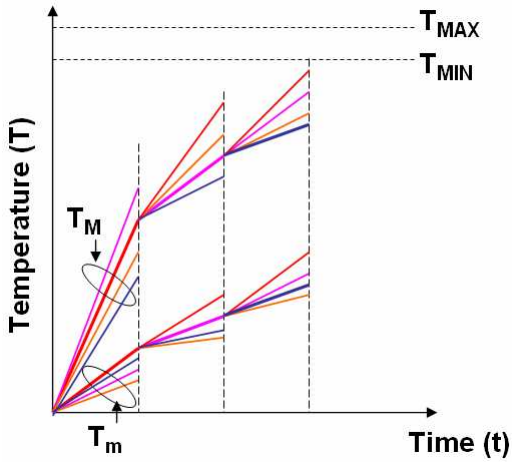

Fig. 3.2. Operation of optimization algorithm by choosing the best combination of specified functions.

results from using this optimal set of parameters is then saved and used as the basis for the next heating step. An illustration of this algorithm is shown in Fig. 3.2.

The tested model configurations used in the optimization procedure are chosen based on the analysis used to determine the design variables. Specifically, after we have chosen the set of parameters which most dramatically affect the resulting temperature field, we identify the most complementary heating patterns, that is, those which provide the most uniform pattern when combined. The values for the design variables corresponding to these complementary heating patterns are then used to determine the set of all configurations to be tested in the optimization procedure.

In the implementation of this developed optimization algorithm, we measure the effect on the temperature field by calculating and observing changes in the dissipated power pattern. This method is chosen because the dissipated power can be computed faster and provides a more accurate description of the heating distribution since it does not take heat diffusion into account.

The optimization is performed using each heating step as a constant predefined number, except when the maximum temperature exceeds the prescribed threshold. In this situation, the heating time is reduced so that the maximum temperature equals the threshold. Pulsing MW power is supposed to back up the process in order to let heat diffusion reach the cold spots not addressed by the MW heating controlled by the design variables.

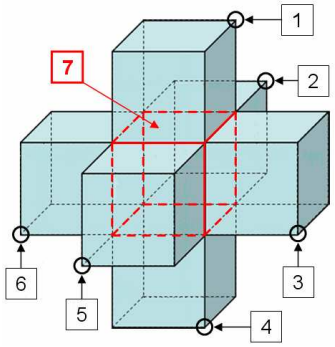

Figure 3.3. Illustration of adjacent pairs of FDTD cells in computation of the average squared temperature deviation. Possible temperature pairs are (T_1, T_7), (T_2, T_7), (T_3, T_7), (T_4, T_7), (T_5, T_7), and (T_6, T_7).

$T_1^{(1)}$	$T_2^{(1)}$	•••	$T_n^{(1)}$
$T_1^{(2)}$	$T_2^{(2)}$	•••	$T_n^{(2)}$

Figure 3.4 Illustration of two rows of adjacent FDTD cells.

3.4 Measuring the Uniformity of Microwave-Induced Temperature Fields

Currently, as discussed previously in Chapter 1, there is no commonly accepted standard definition for the uniformity of MW-induced temperature fields. In this project, uniformity is measured as the average squared temperature deviation corresponding to all neighboring pairs of FDTD cells which represent the heated material:

$$U = \frac{1}{N}\sum_{i=1}^{N}(T_i^{(1)} - T_i^{(2)})^2 \tag{17}$$

where each $(T_i^{(1)}, T_i^{(2)})$ represents the temperature values corresponding to the *i*th distinct pair of adjacent FDTD cells (Fig. 3.3), and *N* is the total number of distinct pairs.

The method used to compute this sum relies on the structure of the FDTD mesh. For every set of adjacent cells in a chosen direction, we compute the contribution by expanding the corresponding terms from the total sum:

$$\sum_{i=1}^{n}(T_i^{(1)} - T_i^{(2)})^2 = \begin{bmatrix} T_1^{(1)} \\ T_2^{(1)} \\ \vdots \\ T_n^{(1)} \end{bmatrix}^T \begin{bmatrix} T_1^{(1)} \\ T_2^{(1)} \\ \vdots \\ T_n^{(1)} \end{bmatrix} + \begin{bmatrix} T_1^{(2)} \\ T_2^{(2)} \\ \vdots \\ T_n^{(2)} \end{bmatrix}^T \begin{bmatrix} T_1^{(2)} \\ T_2^{(2)} \\ \vdots \\ T_n^{(2)} \end{bmatrix} - 2 \cdot \begin{bmatrix} T_1^{(1)} \\ T_2^{(1)} \\ \vdots \\ T_n^{(1)} \end{bmatrix}^T \begin{bmatrix} T_1^{(2)} \\ T_2^{(2)} \\ \vdots \\ T_n^{(2)} \end{bmatrix} \tag{18}$$

where *n* is the number of cells in the chosen direction as illustrated in Fig. 3.4.

The developed optimization algorithm is implemented as series of a *MATLAB* scripts. The simulations are performed and controlled within the *MATLAB* environment calling *QW-3D* and *QW-BHM* from the command line when necessary. Once uniformity has been achieved, the code produces a description of the optimal MW heating process.

Chapter 4

Numerical Results

This chapter presents a detailed description of the entire optimization process applied to two modeled MW heating systems. Additional examples are presented at the conclusion of the chapter to further illustrate the potential effectiveness of the method.

4.1 Material Parameters Data and Design Variables

Temperature dependent data for electric and thermal material parameters does not always exist for a given material. This is due to the difficulties involved in accurately measuring the dielectric constant and the loss factor which can depend substantially on both temperature and the frequency of the electromagnetic field.

In each modeled system, the frequency of the EM field is 915 MHz, and the heated material is chosen to be raw beef. The required temperature-dependent data on this load is available in literature and is reproduced in Table 4.1.

The same design variables are used in the optimization procedure for both modeled systems. We consider the excitation setting for the system and the position of load as the design variables, which are justified by the following considerations. Different excitations result in different orientations of the electric

Table 4.1. Temperature-Dependent Material Parameters of the Load (Raw Beef) [To, et al, 1974; Datta, 2001]

Temp., C	Enthalpy [J/cm³]	Dielectric constant	Loss factor	Specific heat [J/(gC)]	Density [g/cm³]	Heat conductivity [W/(cmC)]
20	0	55.3	1.129	3.63	1.06	0.0069
40	77.0	53.7	1.264	3.63	1.06	0.0069
60	153.9	52.0	1.400	3.63	1.06	0.0069
130	423.3	46.2	1.873	3.63	1.06	0.0069

field in the feed, which, in turn, has a direct impact on the heating pattern. It is also known from practice that the position of the load may have a dramatic effect on the heating pattern – typical household microwave ovens commonly take advantage of this fact by rotating the heated material.

In all presented uniformity simulations, the minimum goal temperature, T_{MIN}, is chosen to be 60°C and the maximum threshold temperature, T_{MAX}, is 70°C.

4.2 Scenario A: Two Feed System

The MW system consists of a rectangular cavity fed by two rectangular waveguides, one positioned directly above and one positioned directly to the side of the cavity. Both feeds are centered with respect to the adjacent cavity walls. The load is a rectangular block of raw beef positioned in the center of the cavity as shown in Fig. 4.1. All dimensions of the system are displayed in Table 4.2.

4.2.1 Results of "Static" Microwave Heating

We first simulate the "static" heating pattern for the system in its base configuration with the load centered in the *xy*-plane and elevated 75 mm above the bottom of the cavity. The extreme variability of the resulting heating pattern shown in Fig. 4.2 indicates that the desired level of uniformity cannot be achieved simply by

processing the load in the system as it is. We hence consider applying a pulsing regime to the given scenario as an attempt to reach the desired level of uniformity.

4.2.2 Reaching Uniformity via Microwave Pulsing

The developed MW pulsing regime is applied to the system in its based configuration. MW power is turned off when T_M reaches 70°C and resumes when T_M has relaxed below 68°C, as illustrated by the time characteristic corresponding to the simulated process shown in Fig. 4.3. The fact that the desired level of uniformity has been reached is illustrated by the cross-sections of the final temperature field shown in Fig. 4.4. However, the time-to-uniformity is nearly two hours which is much too high for this regime to be considered for practical application. This result will serve as a reference point for measuring the success of the optimization procedure in terms of minimizing t_u.

4.2.3 Testing Design Variables

We now consider testing the effectiveness of each design variable, excitation and load position, in terms of the capability to dramatically affect the temperature field by calculating the dissipated power for a number of combinations of settings. Once corresponding patterns have been obtained, the most complementary fields of dissipated power are identified and the corresponding design variable settings are used as the available system configurations in the related optimization procedure.

We assume that the possible excitations in each port are the TE_{10} (dominant) mode, TE_{01} (high-order) mode, or simultaneous application of both modes with a phase shift between them ($\alpha = 0^\circ$ or $\alpha = 90^\circ$) (Fig. 4.5). Possible *x*-positions of the load are taken to be 0 and 130 mm, possible *y*-positions for the load 0 and 100 mm, and possible *z*-positions for the load 10, 75, and 140 mm (see Fig. 4.6). Simulation results are displayed only for specific combinations of these design variables.

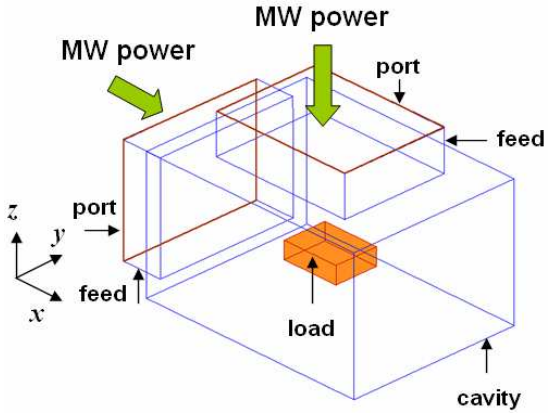

Fig. 4.1. General view of the two-feed cavity.

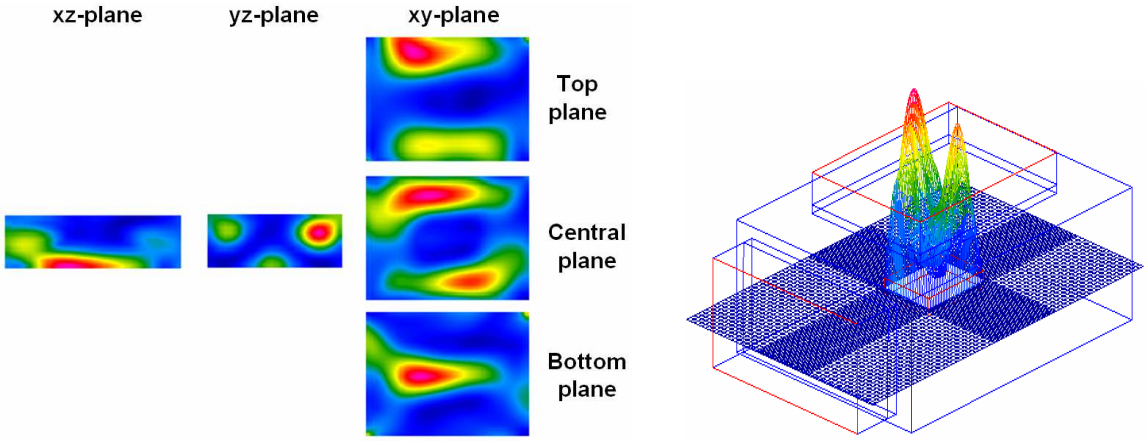

(a) (b)

Fig. 4.2. Computed "static" MW heating in the two-feed cavity (Fig. 4.1) excited by the TE_{10} modes in each feed: patterns of dissipated power in specific coordinate planes of the load (a) and the hilltop view of the pattern in the central *xy*-plane (b).

Table 4.2. Parameters of the MW System in Figure 4.1

Frequency, MHz	915
Power, kW	1
Cavity size, mm	400 x 264 x 180
Load size, mm	100 x 76 x 30
Feed size, mm	RW975: 248 x 124 x 70

Top, central, and bottom horizontal planes of selected dissipated power patterns are displayed in Fig. 4.7 corresponding to the configurations listed in Table 4.3. Based on the obtained results, the pairs of dissipated power patterns which appear the most complementary are Fig. 4.7 (c), (d) and Fig. 4.7 (e), (f). Hence, the combinations of design variables used in the related optimization procedure are chosen to be:

- Top feed, TE_{10} mode, load on the bottom (z =10 mm), centered ($x = y = 0$),
- Top feed, TE_{01} mode, load on the bottom (z =10 mm), centered ($x = y = 0$),
- Circular polarization in both feeds, load on the top (z =140 mm), cornered (x = 130, y = 80 mm), and
- Circular polarization in both feeds, load on the bottom (z = 10 mm), cornered (x = 130, y = 80 mm).

4.2.4 Optimization Results

A picture illustrating the details of the optimization procedure is displayed in Fig. 4.8. The minimum and maximum temperatures corresponding to each tested configuration are shown along with the optimal choice at each given time. The optimization procedure was performed for the given configurations using 10 s heating time-steps. MW power is turned off when T_M reaches 70^{o}C and resumes when T_M has relaxed below 68^{o}C, as illustrated by the time characteristic corresponding to the optimal process presented in Fig. 4.9. Uniformity is reached in nearly 30 minutes which is a 3.7 times reduction in time-to-uniformity compared to the pulsing regime.

Top, central, and bottom horizontal planes of the temperature field are displayed at various times during the simulation in Fig. 4.10. These pictures illustrate how uniformity of the temperature field is reached during the simulation. A detailed description of the optimal process is given in Table 4.4. Whenever the system is changed, the appropriate time is provided along with the new settings of the system.

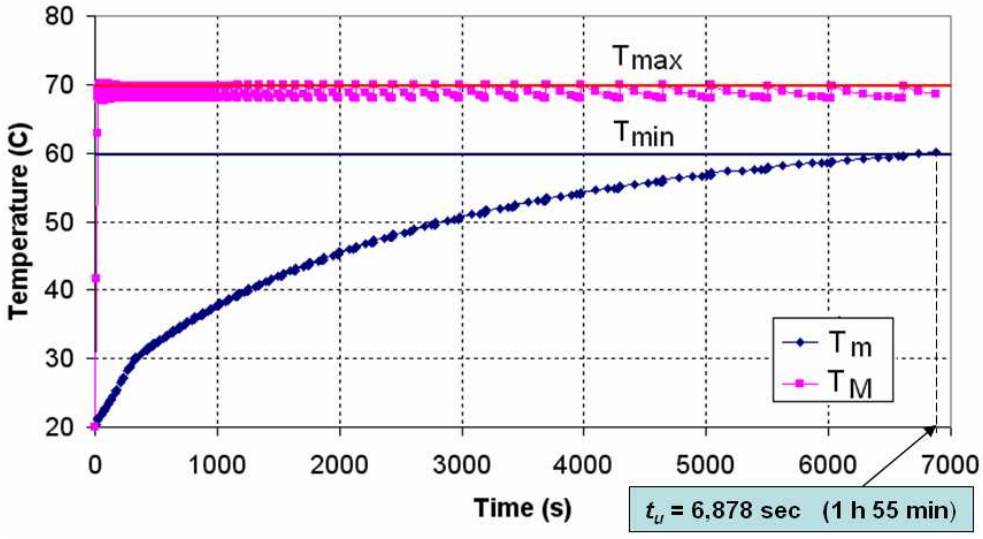

Fig. 4.3. Time characteristic of the heating process for the two-feed cavity under a pulsing regime alone (allowable relaxation of T_M from T_{MAX} to 68°C).

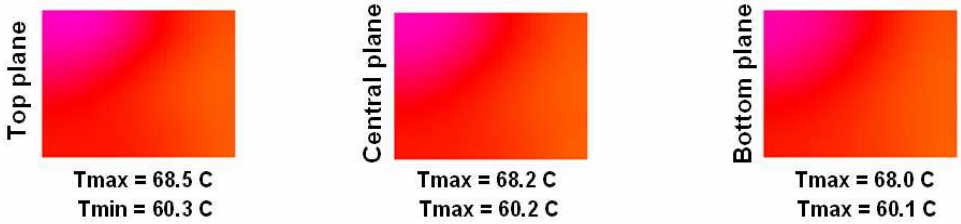

Fig. 4.4. Temperature patterns in specific horizontal planes of the load heated in a pulsing regime (Fig. 4.3.) at t_u; normalized to maximum temperature in all layers.

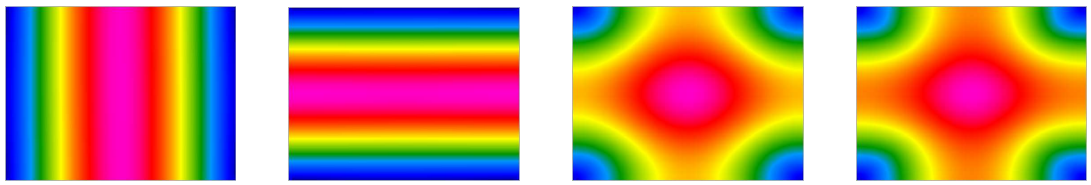

(a) (b) (c) (d)

Fig. 4.5. Possible electric field patterns in exciting feeds of the two-feed cavity: TE_{10} mode (a), TE_{01} mode (b), both TE_{10}, TE_{01} modes with no phase shift (c), and both TE_{10}, TE_{01} modes with a 90° phase shift (d).

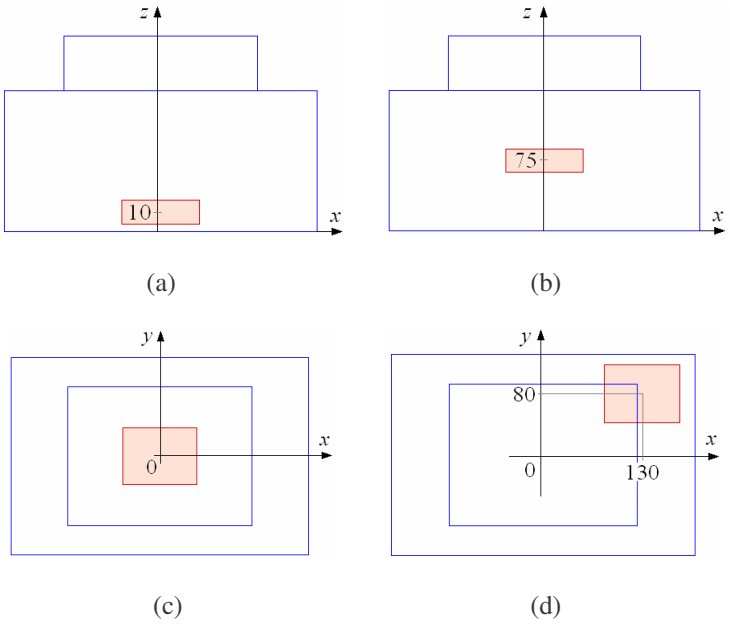

Fig. 4.6. Possible positions of the load in the two-feed cavity: at the level z = 10 (a) and 75 mm (b) above the bottom, in the cavity's center (x,y) = (0,0 mm) (c), and shifted in the cavity's corner (x,y) = (130,80 mm) (d).

Table 4.3. Parameters of the Two-Feed System Tested for Specifying the Design Variables

Patterns in Fig. 4.7	Feed, excitation, position of the load
(a)	Side feed, **TE_{10} mode**, load on the bottom (z =10 mm), centered ($x = y = 0$)
(b)	Side feed, **TE_{01} mode**, load on the bottom (z =10 mm), centered ($x = y = 0$)
(c)	Top feed, **TE_{10} mode**, load on the bottom (z =10 mm), centered ($x = y = 0$)
(d)	Top feed, **TE_{01} mode**, load on the bottom (z =10 mm), centered ($x = y = 0$)
(e)	Circular polarization in both feeds, **load on the top (z =140 mm)**, cornered (x = 130, y = 80mm)
(f)	Circular polarization in both feeds, **load on the bottom (z = 10mm)**, cornered (x = 130, y = 80mm)
(g)	Circular polarization in both feeds, **load in the top (z = 140 mm)**, centered ($x = y = 0$)
(h)	Circular polarizations in both feeds, **load in the center (z = 75mm)**, centered ($x = y = 0$)
(i)	Circular polarizations in both feeds, **load on the bottom (z = 10 mm)**, centered ($x = y = 0$)

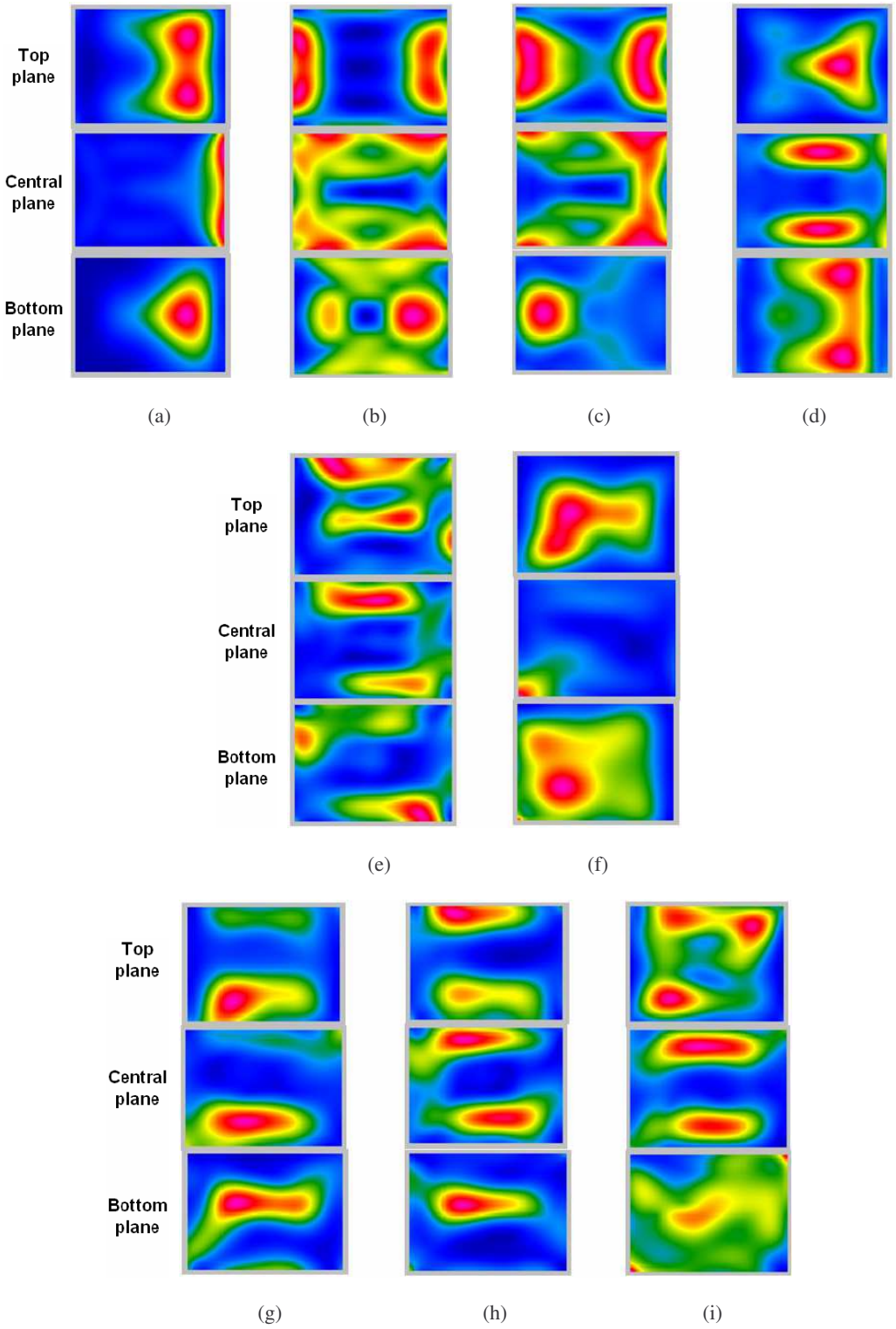

Fig. 4.7. Dissipated power patterns in specific horizontal planes of the load heated in the two-feed system in accordance with Table 4.3.

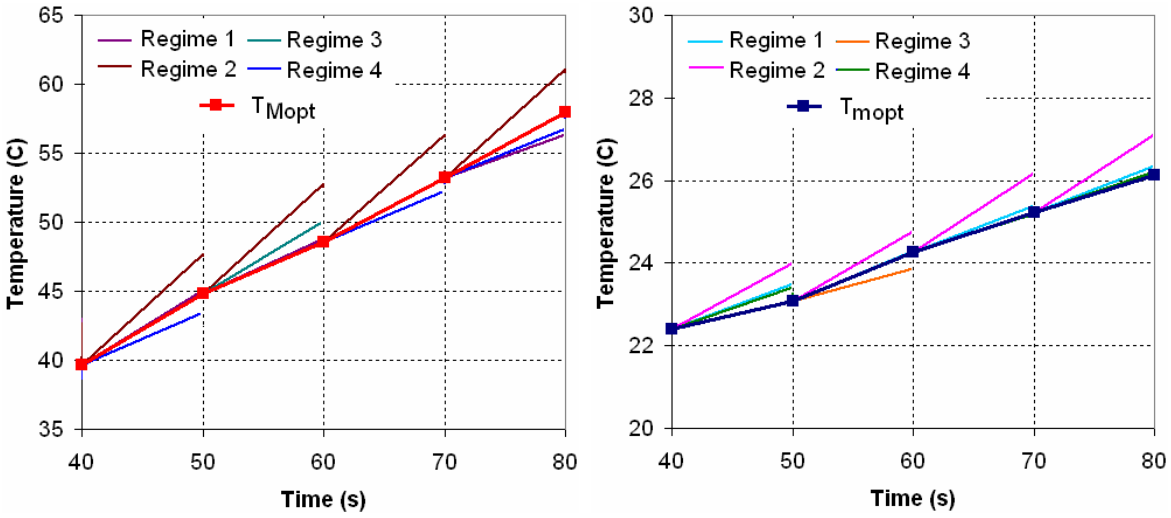

(a) (b)

Fig. 4.8. Performance of the optimization algorithm from 40-80 s in choosing best regimes for maximum (a) and minimum temperatures of the load (b). Regime 1: circular polarization in both feeds, (x,y,z) = (130,100,140 mm). Regime 2: circular polarization in both feeds, (x,y,z) = (130,100,10 mm). Regime 3: TE_{10} mode in top feed, (x,y,z) = (0,0,10 mm). Regime 4: TE_{01} mode in top feed, (x,y,z) = (0,0,10 mm).

4.3 Scenario B: One Feed System

The MW system consists of a rectangular cavity fed by a rectangular waveguide positioned and centered directly above the cavity. The load is a rectangular block of raw beef positioned in the center of the cavity (Fig. 4.11). All dimensions of the system are displayed in Table 4.5.

4.3.1 Results of "Static" Microwave Heating

We first obtain "static" heating results for the system in its base configuration with the load centered in the *xy*-plane and elevated 75 mm above the bottom of the cavity, which are shown in Fig. 4.12. Similar results

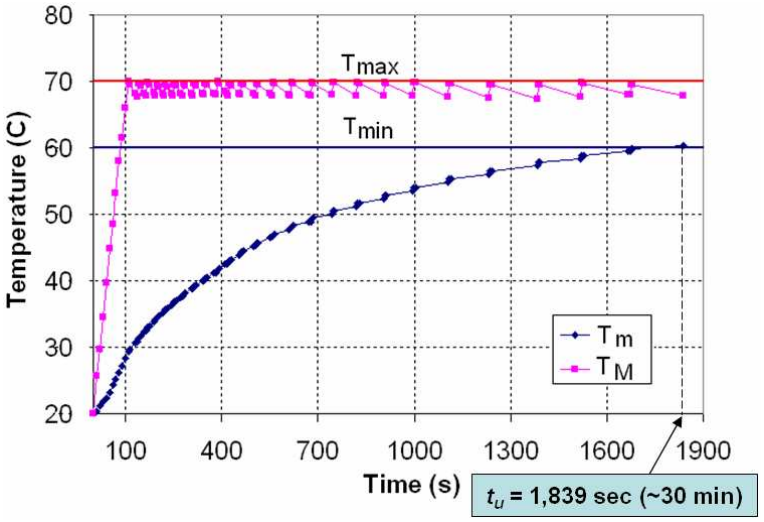

Fig. 4.9. Time characteristic of the optimal heating process for the two-feed cavity (allowable relaxation of T_M from T_{MAX} to 68°C).

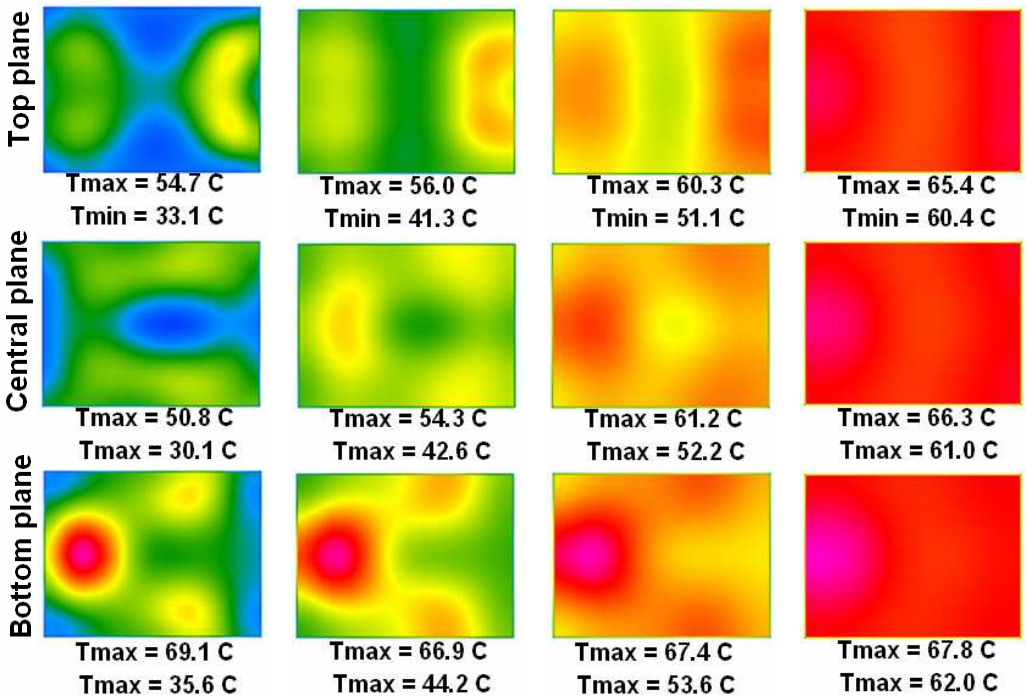

(a) (b) (c) (d)

Fig. 4.10. Optimal heating process for two-feed cavity: intermediate and resulting temperature patterns in specific horizontal planes of the load after 109 s (a), 344 s (b), 742 s (c) and t_u = 1,839 s (d).

Table 4.4. Detailed Description of the Optimal MW Heating Process for the Two-Feed Cavity

- Two different types of excitation:
  - **(V)** TE_{10} mode
  - **(H)** TE_{01} mode
- Two positions of the load:
  - **(a)** z = 10 mm
  - **(b)** z = 140 mm

Initial settings: **(V)** & (a)

0 s:	Begin heating	**282 s**:	Relax system	**742 s**:	Resume: **(V)**
10 s:	Switch to **(H)**	**310 s**:	Resume: **(V)**	**746 s**:	Relax system
20 s:	Switch to **(V)**	**314 s**:	Relax system	**819 s**:	Resume: **(V)**
50 s:	Switch to **(H)**	**344 s**:	Resume: **(V)**	**823 s**:	Relax system
60 s:	Switch to **(V)**	**348 s**:	Relax system	**904 s**:	Resume: **(V)**
80 s:	Switch to **(H)**	**381 s**:	Resume: **(H)**	**908 s**:	Relax system
90 s:	Switch to **(V)**	**387 s**:	Relax system	**995 s**:	Resume: **(V)**
109 s:	Relax system	**420 s**:	Resume: **(V)**	**999 s**:	Relax system
136 s:	Resume: **(V)**	**424 s**:	Relax system	**1105 s**:	Resume: **(V)**
141 s:	Relax system	**458 s**:	Resume: **(V)**	**1109 s**:	Relax system
164 s:	Resume: **(V)**	**462 s**:	Relax system	**1233 s**:	Resume: **(V)**
169 s:	Relax system	**505 s**:	Resume: **(V)**	**1237 s**:	Relax system
194 s:	Resume: **(V)**	**509 s**:	Relax system	**1382 s**:	Resume: (V)
198 s:	Relax system	**556 s**:	Resume: (V)	**1386 s**:	Relax system
220 s:	Resume: **(V)**	**560 s**:	Relax system	**1519 s**:	Resume: **(V)**
224 s:	Relax system	**614 s**:	Resume: **(V)**	**1523 s**:	Relax system
248 s:	Resume: **(V)**	**618 s**:	Relax system	**1672 s**:	Resume: **(V)**
252 s:	Relax system	**677 s**:	Resume: **(V)**	**1675 s**:	Relax system
278 s:	Resume: **(V)**	**681 s**:	Relax system	**1839 s**:	***Finished***

for the dissipated power were obtained by Huo and Lu [2005] which can be used as a source of validation for the model developed for this scenario. As in the previous example, the extreme variability of the resulting heating pattern indicates that the desired level of uniformity cannot be achieved by processing the load in the system as it is. So we consider applying a pulsing regime to the given scenario as an attempt to reach the desired level of uniformity.

4.3.2 Reaching Uniformity via Microwave Pulsing

Initial uniformity results are obtained by applying a pulsing regime to the given system in its base configuration. MW power is turned off when T_M reaches 70°C and resumes when T_M has relaxed below 68°C, as illustrated by the time characteristic corresponding to the simulated process, see Fig. 4.13. The fact that the desired level of uniformity has been reached is illustrated by the cross-sections of the final temperature field shown in Fig. 4.14. However, the time-to-uniformity is nearly 103 minutes which is, again, much too high for

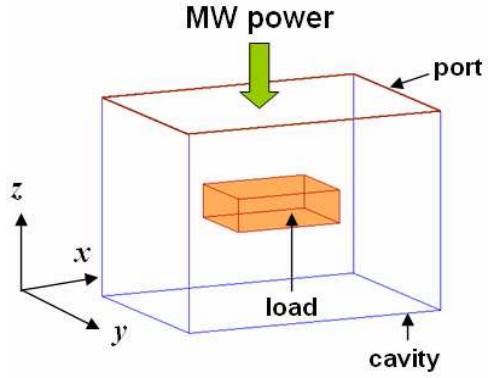

Fig. 4.11. General view of the one-feed cavity.

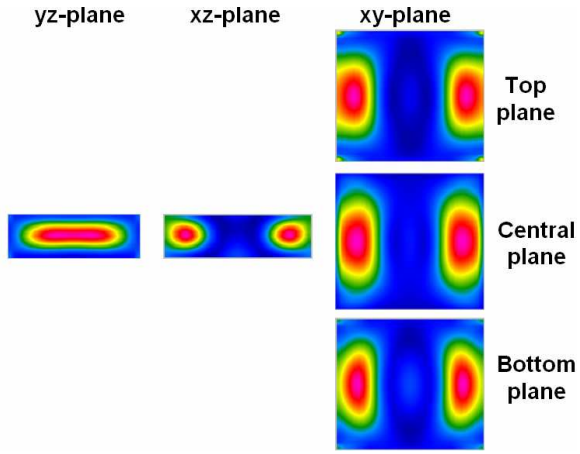

Fig. 4.12. Computed "static" MW heating in the one-feed cavity (Fig. 4.11) excited by the TE_{10} mode: patterns of dissipated power in specific coordinate planes of the load.

Table 4.5. Parameters of the MW System in Figure 4.11

Frequency, MHz	915
Power, kW	1
Cavity size, mm	248 x 124 x 180
Load size, mm	85 x 76 x 25
Feed size, mm	RW975: 248 x 124

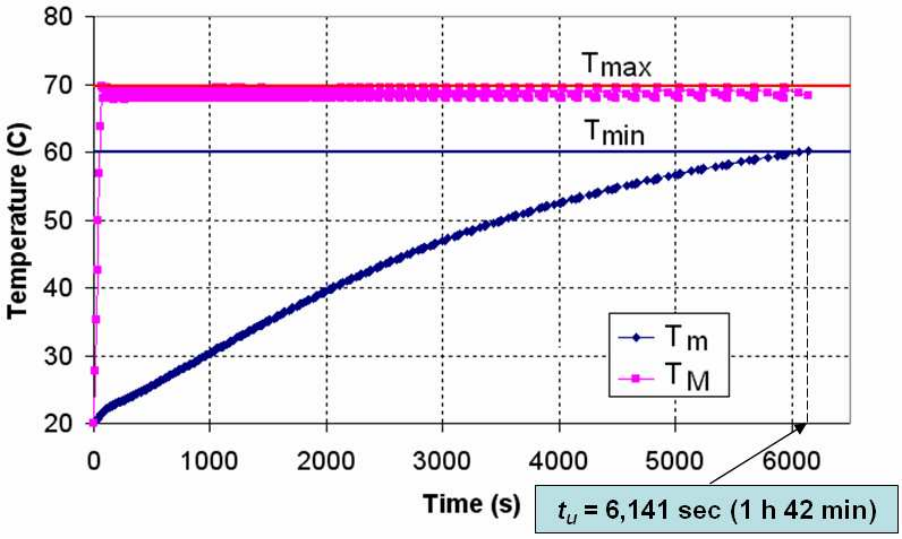

Fig. 4.13. Time characteristic of the heating process for the one-feed cavity under a pulsing regime alone (allowable relaxation of T_M from T_{MAX} to 68°C).

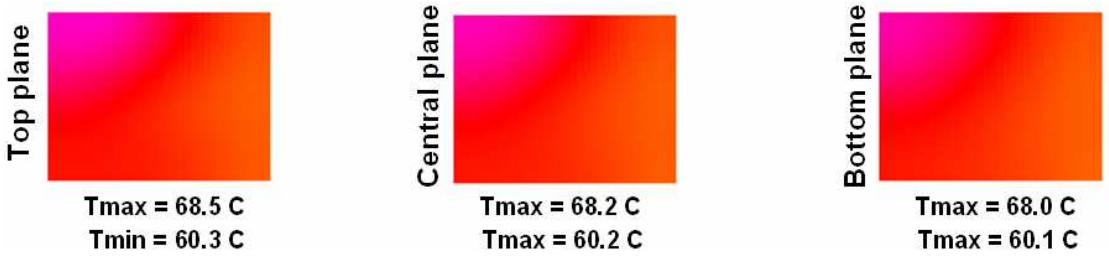

Fig. 4.14. Temperature patterns in specific horizontal planes of the load heated in a pulsing regime (Fig. 4.13) at t_u; normalized to maximum temperature in all layers.

this regime to be considered for practical application. These results will similarly serve as a reference point for measuring the success of the optimization procedure in terms of minimizing t_u.

4.3.3 Testing Design Variables

We again consider testing the effectiveness of each design variable, excitation and load position, in terms of its capability to dramatically affect the temperature pattern by calculating the dissipated power patterns for a

Table 4.6. Parameters of the One-Feed System Tested for Specifying the Design Variables

Patterns in Fig. 4.15	Feed, excitation, position of the load
(a)	**TE_{10} mode**, load in the middle of the cavity (z = 75 mm), centered ($x = y = 0$)
(b)	**TE_{01} mode**, load in the middle of the cavity (z = 75 mm), centered ($x = y = 0$)
(c)	TE_{10} mode, **load in the middle of the cavity (z = 75 mm)**, centered ($x = y = 0$)
(d)	TE_{10} mode, **load on the bottom of the cavity (z = 10 mm)**, centered ($x = y = 0$)
(e)	TE_{10} mode, load on the bottom of the cavity (z = 10 mm), **centered ($x = y = 0$)**
(f)	TE_{10} mode, load on the bottom of the cavity (z = 10 mm), **cornered (x = 70, y = 40 mm)**
(g)	TE_{01} mode, load on the bottom of the cavity (z = 10 mm), **centered ($x = y = 0$)**
(h)	TE_{01} mode, load on the bottom of the cavity (z = 10 mm), **cornered (x = 70, y = 40 mm)**
(i)	TE_{01} mode**, load in the middle of the cavity (z = 75 mm)**, centered ($x = y = 0$)
(j)	TE_{01} mode**, load on the bottom of the cavity (z = 10 mm),** centered ($x = y = 0$)
(k)	Both TE_{10} and TE_{01} modes **with 0 phase shift between them**, load in the middle of the cavity (z = 75 mm), centered ($x = y = 0$)
(l)	Both TE_{10} and TE_{01} modes **with 90^o phase shift between them**, load in the middle of the cavity (z = 75 mm), centered ($x = y = 0$)
(m)	Both TE_{10} and TE_{01} modes with 90^o phase shift between them, **load on the bottom of the cavity (z = 10 mm)**, centered ($x = y = 0$)
(n)	Both TE_{10} and TE_{01} modes with 90^o phase shift between them, **load in the middle of the cavity (z = 75 mm)**, centered ($x = y = 0$)

number of combinations of settings for the excitation and load position. As in the previous example, once these patterns have been obtained, the most complementary dissipated power patterns are identified and the corresponding design variable settings are used as the available system configurations in the related optimization procedure.

We assume that the possible excitations are the TE_{10} (dominant) mode, TE_{01} (high-order) mode, or simultaneous application of both modes with a phase shift between them ($\alpha = 0^\circ$ or $\alpha = 90^\circ$). Possible x-positions of the load are taken to be 0 and 70 mm, possible y-positions for the load 0 and 40 mm, and possible z-positions for the load 10 and 75 mm. Simulation results are displayed only for specific combinations of these design variables.

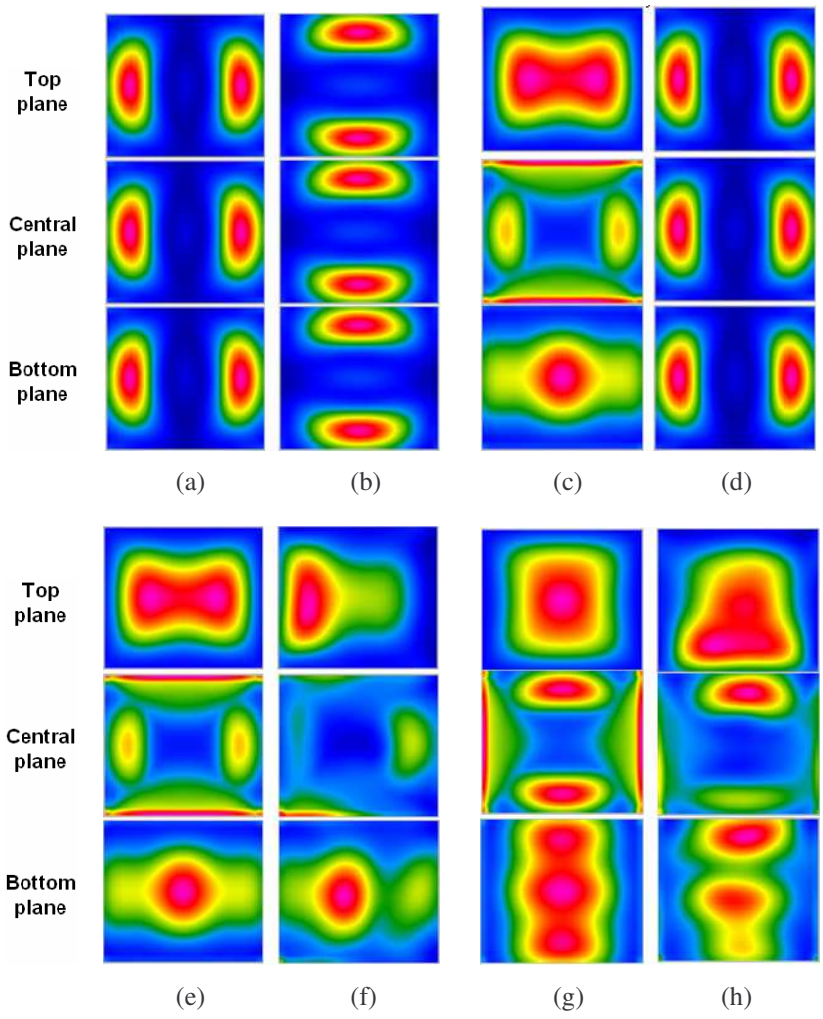

Fig. 4.15.

Top, central, and bottom horizontal planes of selected dissipated power patterns are displayed in Fig. 4.15 corresponding to the configurations listed in Table 4.6. Based on the obtained results, the most complementary heating patterns seem to be 4.15 (c), (d), 4.15 (i), (j), and 4.15 (m), (n). Hence, the combinations of design variables used in the related optimization procedure are chosen to be:

- TE_{10} mode, load in the middle of the cavity (z = 75 mm), centered ($x = y = 0$),
- TE_{10} mode, load on the bottom of the cavity (z = 10 mm), centered ($x = y = 0$),
- TE_{01} mode, load in the middle of the cavity (z = 75 mm), centered ($x = y = 0$),

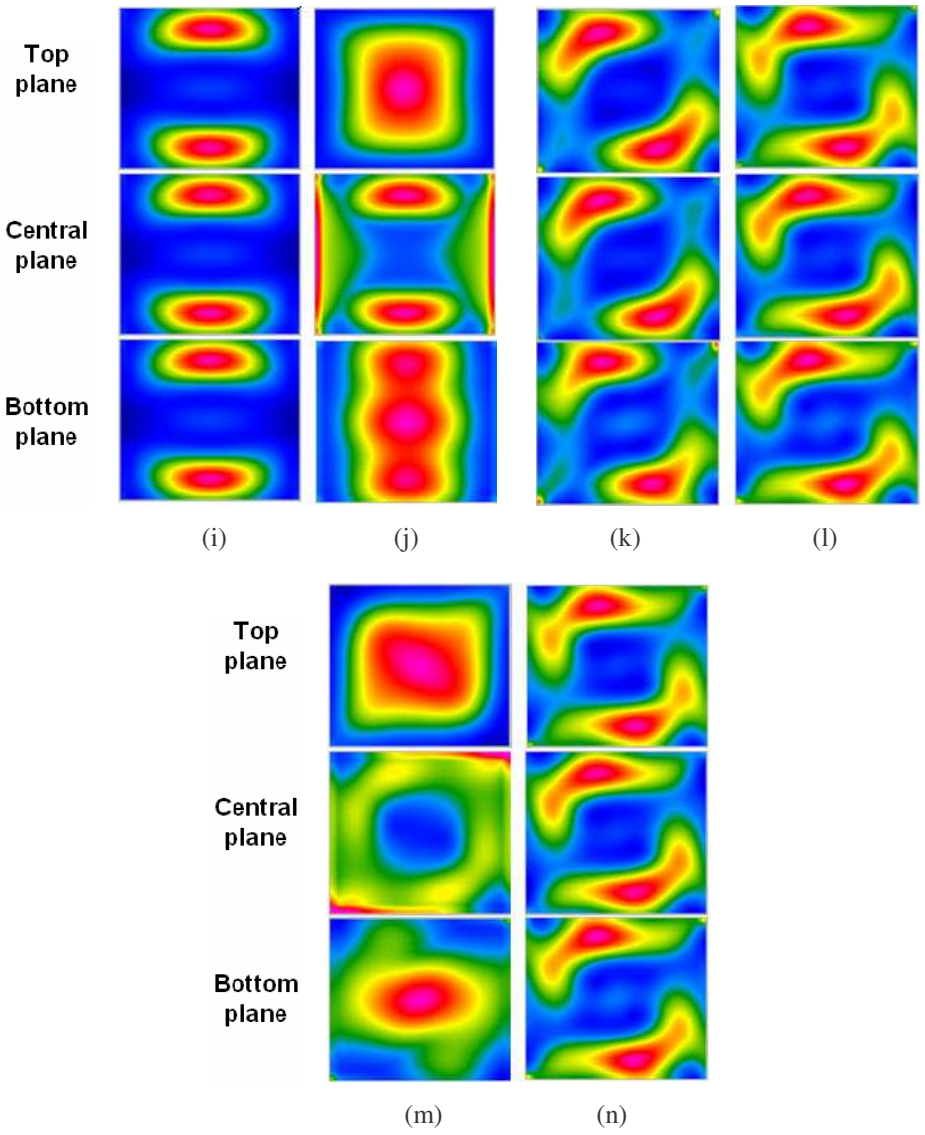

Fig. 4.15 (cont'd). Dissipated power patterns in specific horizontal planes of the load heated in the two-feed system in accordance with Table 4.6.

- TE_{01} mode, load on the bottom of the cavity (z = 10 mm), centered ($x = y = 0$),
- Both TE_{10} and TE_{01} modes with 90° phase shift between them, load on the bottom of the cavity (z = 10 mm), centered ($x = y = 0$), and
- Both TE_{10} and TE_{01} modes with 90° phase shift between them, load in the middle of the cavity (z = 75 mm), centered ($x = y = 0$).

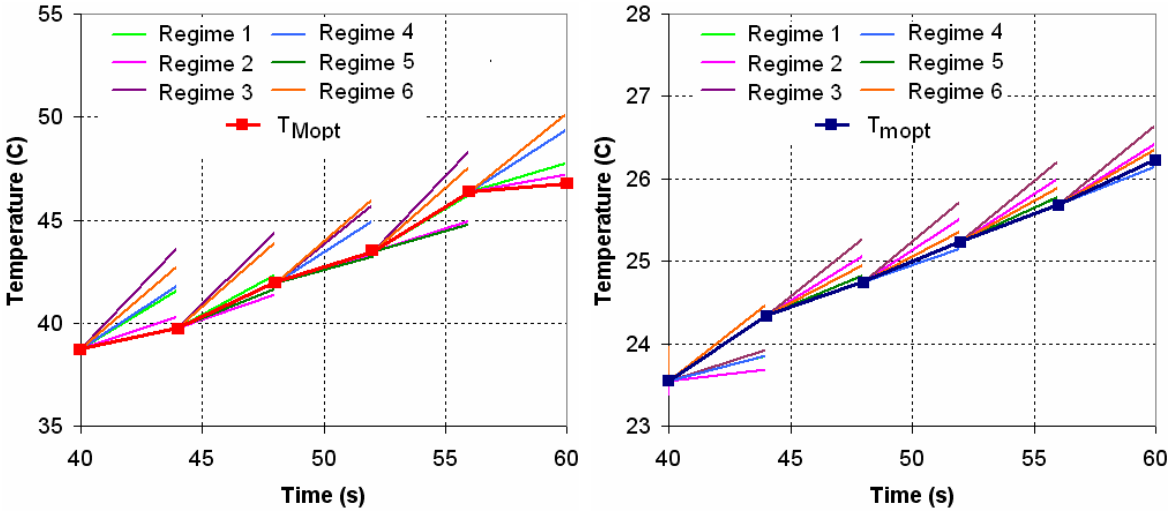

(a) (b)

Fig. 4.16. Performance of the optimization algorithm from 40-60 s in choosing best regime for maximum (a) and minimum temperatures of the load (b). Regime 1: TE_{10} mode, z = 10 mm; Regime 2: TE_{01} mode, z = 10 mm; Regime 3: circular polarization, z = 10 mm; Regime 4: TE_{10} mode, z = 75 mm; Regime 5: TE_{01} mode, z = 75 mm; Regime 6: circular polarization, z = 75 mm.

4.3.4 Optimization Results

A picture illustrating the performance of the optimization procedure is shown in Fig. 4.16. The minimum and maximum temperatures corresponding to each tested configuration are shown along with the optimal choice at each given time. The optimization was performed for the specified configurations using 4 s heating time-steps. MW power is turned off when T_M reaches 70 ^oC and resumes when T_M has relaxed below 68 ^oC, as illustrated by the time characteristic corresponding to the optimal process in Fig. 4.17. Uniformity is reached in 20 minutes which is 5.3 times reduction in time-to-uniformity compared to the pulsing regime.

Top, central, and bottom horizontal planes of the temperature field are displayed at various times in Fig. 4.18. These pictures illustrate how uniformity is reached during the simulation. An alternate visualization of the final temperature is displayed in Fig. 4.19.

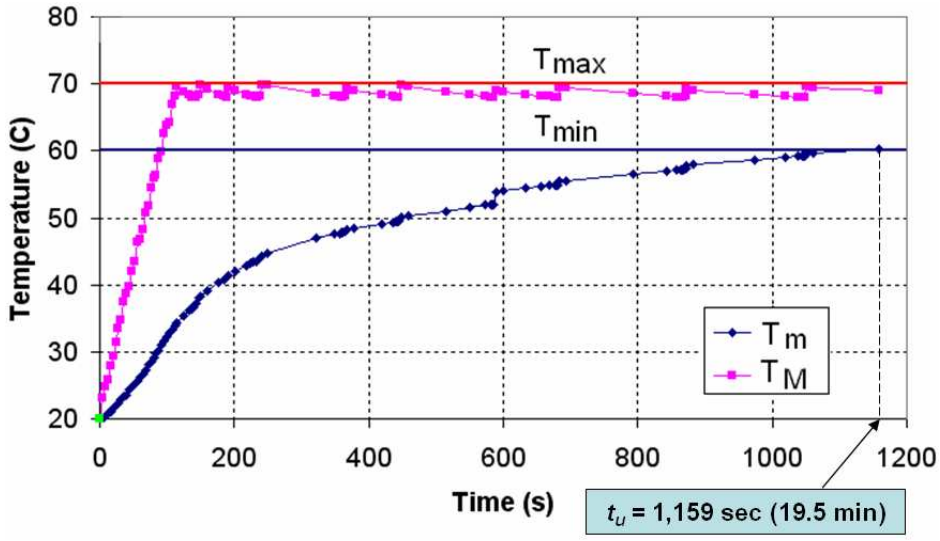

Fig. 4.17. Time characteristic of the optimal heating process for the one-feed cavity (allowable relaxation of T_M from T_{MAX} to 68°C).

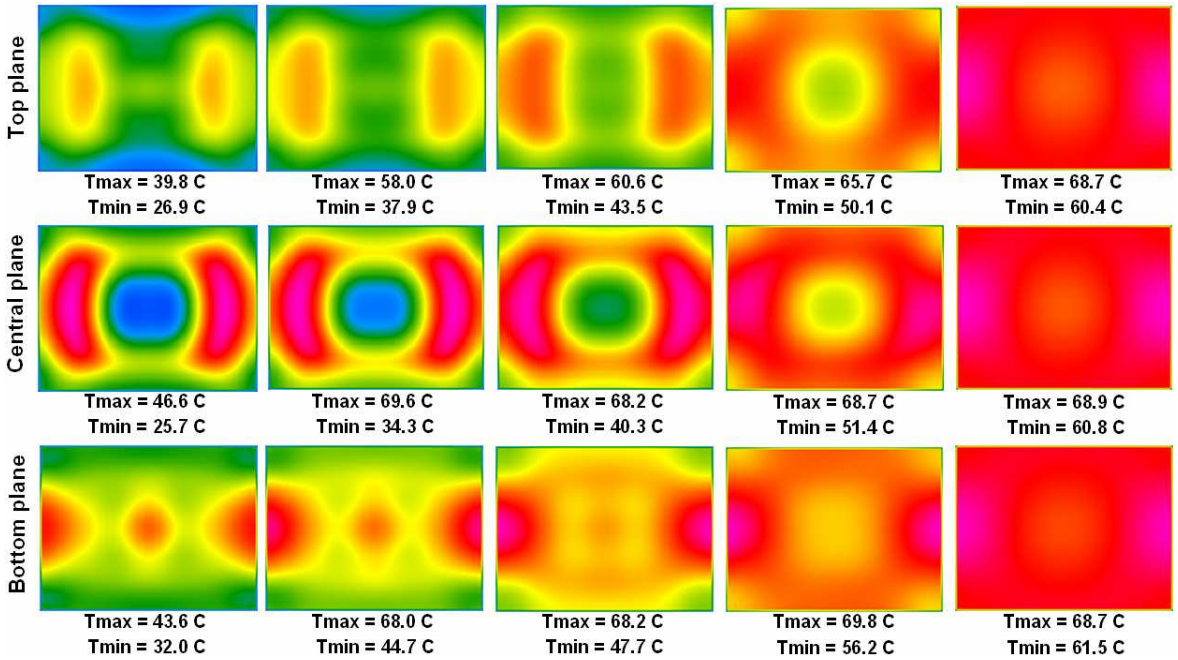

(a) (b) (c) (d) (e)

Fig. 4.18. Optimal heating process for the two-feed cavity: intermediate and resulting temperature patterns in specific horizontal planes of the load after 56 s (a), 114 s (b), 177 s (c), 448 s (d) and t_u = 1,159 s (d).

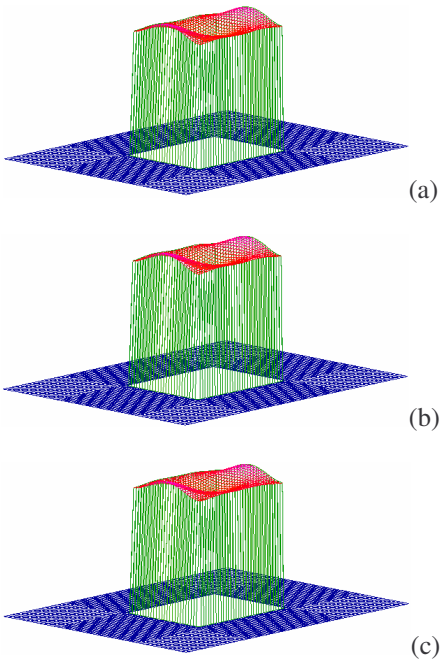

Fig. 4.19. Temperature patterns of Fig. 4.17 (e) in the hill-top format: top plane (a), central plane (b) and bottom plane (c).

Table 4.7. Detailed Description of the Optimal MW Heating Process for the One-Feed Cavity

- Three different types of excitation:
  - **(V)** TE_{10} mode
  - **(H)** TE_{01} mode
  - **(C)** Circular Polarization
- Two positions of the load:
  - **(a)** z = 10 mm
  - **(b)** z = 75 mm

Initial settings: **(V)** & **(b)**

0 s:	Begin heating	**72 s**:	Switch to **(V) & (b)**	**234 s**:	Resume: **(H) & (b)**
4 s:	Switch to **(V) & (a)**	**76 s**	Switch to **(V) & (a)**	**238 s**:	Switch to **(V) & (a)**
8 s:	Switch to **(H) & (b)**	**80 s**:	Switch to **(H) & (b)**	**240 s**:	Relax system
12 s:	Switch to **(V) & (b)**	**84 s**:	Switch to **(V) & (b)**	**362 s**:	Resume: **(H) & (b)**
16 s:	Switch to **(H) & (a)**	**88 s**:	Switch to **(H) & (a)**	**366 s**:	Switch to **(V) & (a)**
20 s:	Switch to **(V) & (a)**	**92 s**:	Switch to **(V) & (b)**	**367 s**:	Relax system
24 s:	Switch to **(V) & (b)**	**96 s**:	Switch to **(V) & (a)**	**444 s**:	Resume: **(V) & (b)**
28 s:	Switch to **(H) & (a)**	**100 s**:	Switch to **(H) & (b)**	**448 s**:	Relax system
32 s:	Switch to **(V) & (b)**	**104 s**:	Switch to **(V) & (b)**	**585 s**:	Resume: **(H) & (a)**
36 s:	Switch to **(V) & (a)**	**108 s**:	Switch to **(V) & (a)**	**589 s**:	Relax system
40 s:	Switch to **(H) & (b)**	**112 s**:	Switch to **(V) & (b)**	**680 s**:	Resume: **(V) & (b)**
44 s:	Switch to **(V) & (b)**	**114 s**:	Relax system	**683 s**:	Relax system
48 s:	Switch to **(V) & (a)**	**140 s**:	Resume: **(H) & (b)**	**867 s**:	Resume: **(H) & (b)**
52 s:	Switch to **(V) & (b)**	**144 s**:	Switch to **(H) & (a)**	**871 s**:	Switch to **(V) & (a)**
56 s:	Switch to **(H) & (b)**	**148 s**:	Switch to **(V) & (b)**	**872 s**:	Relax system
60 s:	Switch to **(V) & (a)**	**150 s**:	Relax system	**1048 s**:	Resume: **(V) & (b)**
64 s:	Switch to **(V) & (b)**	**189 s**:	Resume: **(V) & (b)**	**1051 s**:	Relax system
68 s:	Switch to **(H) & (a)**	**191 s**:	Relax system	**1159 s**:	*Finished*

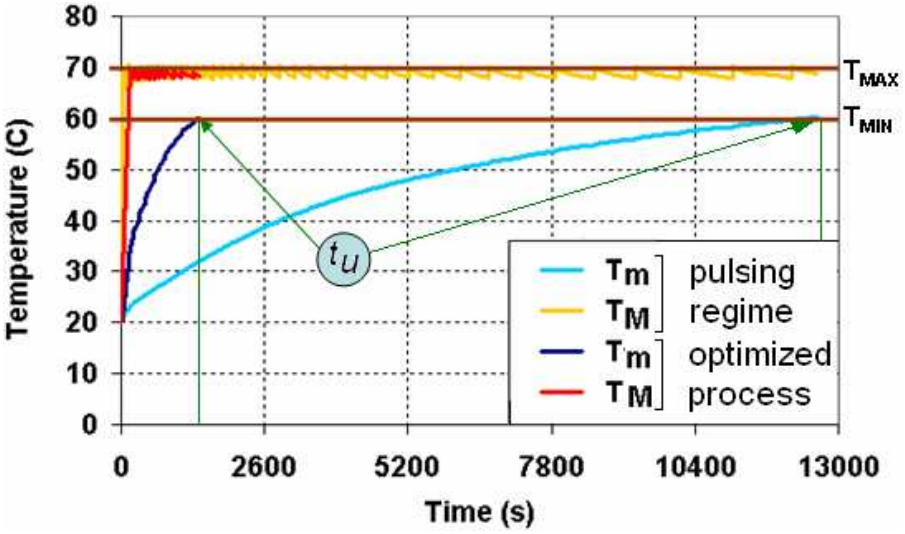

Fig. 4.20. Time characteristic of the optimal heating process for the two-feed cavity in comparison with heating under a pulsing regime alone (allowable relaxation of T_M from T_{MAX} to 68°C). Pulsing regime: 1 kW, TE_{01} mode (side waveguide), cornered load (x,y) = (130,100 mm); optimization's design variable: excitation.

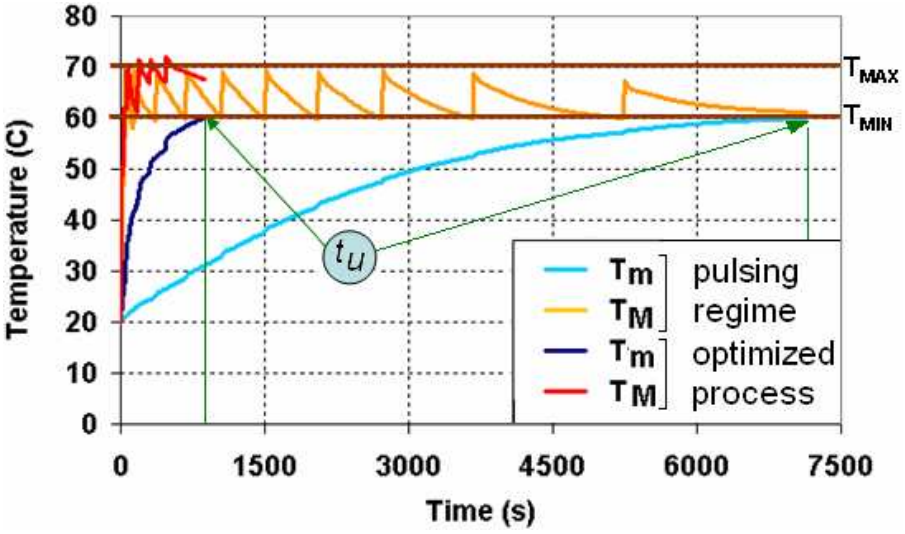

Fig. 4.21. Time characteristic of the optimal heating process for the one-feed cavity in comparison with heating under a pulsing regime alone (allowable relaxation of T_M from T_{MAX} to 60°C). Pulsing regime: 1 kW, TE_{10} mode, centered load; optimization's design variables: excitation, load position, input power.

A detailed description of the optimal process is shown in Table 4.7. Whenever the system is changed, the appropriate time is provided along with the new settings.

4.4 Additional Examples

For each developed system, one additional optimization was performed. For scenario A, a pulsing regime was applied to the given system using the TE_{01} mode in the side port as the excitation and x, y, z = (130, 100, 75 mm) as the position. MW power is turned off when T_M reaches 70°C and resumes when T_M has relaxed below 68°C. The only design variable chosen to be used in the related optimization procedure was excitation. The optimization procedure was performed using 10 s heating time-steps and the same relaxation conditions as in the pulsing regime. The results obtained from this optimization indicate that time-to-uniformity is reduced from 12,625 s to 1,428 s which is an 8.8 times reduction in time. A comparison between the time characteristics of the pulsing and optimal processes is shown in Fig. 4.20.

For scenario B, a pulsing regime was applied to the given system using the TE_{10} mode as the excitation and x, y, z = (0, 0, 75 mm) as the position. MW power is turned off when T_M reaches 70°C and resumes when T_M has relaxed below 60°C. The design variables chosen to be used in the related optimization procedure were the level of input power, excitation, and load position. The optimization procedure was performed using 4 s heating time-steps in which MW power is turned off when T_M reaches 70°C and resumes when T_M has relaxed below 68°C. The results show that time-to-uniformity is reduced from 7,144 s to 874 s which is an 8.2 times reduction in time. A comparison between the time characteristics of the pulsing and optimal processes is shown in Fig. 4.21. These results illustrate both the effectiveness of the optimization procedure and the difficulties of the problem.

Chapter 5

Conclusions

An original modeling-based technique for solving the problem of MW heating uniformity has been proposed.

Accurate numerical simulation of MW heating processes is achieved by developing a suitable mathematical model of the problem and solving the governing system of coupled equations using an appropriate solution algorithm. Implementation of this algorithm is provided by the full-wave electromagnetic modeling software *QuickWave-3D* and the *QW-BHM* module, which apply the 3D conformal FDTD method. The concepts of MW heating processes with variable characteristics and MW pulsing have been introduced and corresponding implementations have been provided.

A definition for the optimization problem has been proposed which considers minimizing the time required to reach uniformity in a given MW system. Design variables in the related optimization have been chosen to be the characteristics of the system which produce the most dramatic affect on the heating pattern when changed. The corresponding optimization algorithm applies the concepts of MW heating processes with variable characteristics and MW pulsing to determine the most uniform heating pattern at each simulated time-step where uniformity is measured in terms of properties of the resulting temperature field. The tested model configurations used in the optimization procedure have been chosen based on the idea of complementary heating patterns which are visually identified based on the simulation results used to determine the design variables.

The optimization algorithm and related modeling concepts have been implemented as a combination of *MATLAB* scripts which manipulate *QW-3D* and *QW-BHM* and generate a description of the optimal process. The functionality of the proposed technique has been illustrated by several computational experiments in which time-to-uniformity was reduced by 4 to 8 times.

The results obtained show that the developed optimization technique is limited in its ability to evaluate the potential heating uniformity resulting from the sequential application of different available model configurations because the visual identification process for determining complementary heating patterns makes it difficult to take into account the presence of reflection of the electromagnetic field from the cavity. The level of reflections can both depend significantly on the configuration of the system and play an essential role in the development of efficient MW heating systems [Mechenova and Yakovlev, 2004; Requena-Pérez, et al, 2004; Domínguez-Tortajada, et al, 2005; Murphy and Yakovlev, 2006]. The effectiveness of the optimization procedure can therefore be improved via enhancing the identification process for determining complementary patterns by monitoring and appropriately accounting for the presence of these reflections.

Appendix

Implementations for the advanced simulation regime presented in Fig. 2.6 and the optimization algorithm illustrated in Fig. 3.2 are achieved with the use of a collection of developed MATLAB scripts.

A. Simulation Software

The two main controlling scripts which implement the advanced simulation regime are `QW_Simulate_Prepare.m` and `QW_Simulate_Run.m`. After specifying the details of the MW heating experiment to be simulated by modifying and calling `QW_Simulate_Prepare`, the experiment is performed by calling `QW_Simulate_Run`. When the simulation is finished, `QW_Simulate_Run` returns the time characteristic of the simulated process along with the corresponding operating procedure.

B. Optimization Software

The two main controlling scripts which implement the optimization algorithm are `QW_Optimize_Prepare.m` and `QW_Optimize_Run.m`. After specifying the details of the desired optimization procedure to performed by modifying and calling `QW_Optimize_Prepare`, the optimization is executed by calling `QW_Optimize_Run`. When the optimization is finished, `QW_Optimize_Run`

returns the time characteristic of the optimal MW heating process along with the corresponding operating procedure.

The remaining MATLAB scripts manage important tasks that are frequently performed during the operation of the respective routines. Specifically, these scripts are `QW_write_UDOfile.m`, `QW_write_UDOparams.m`, `QW_run_QWS.m`, `QW_read_HFIfile.m`, `QW_write_HFIfile.m`, `QW_get_CavityData.m`, `QW_get_ModelData.m`, `QW_get_SavedField.m`, `QW_eval_MinMaxTemp.m`, `QW_modify_FieldMesh.m`. and `QW_eval_FieldUniformity.m`. The complete collection of developed scripts consists of over *1800* lines of MATLAB code.

The corresponding MATLAB code is not included in this report as requested by the research sponsor, The Ferrite Company Inc. This developed approach will potentially be used as an industrial tool to design efficient microwave heating systems and hence is considered proprietary information which must be kept confidential.

Bibliography

Alpert, Y. and E. Jerby (1999). Coupled thermal-electromagnetic model for microwave heating of temperature-dependent dielectric media, *IEEE Trans. Plasma Sci.,* 27 (2), pp. 555-562.

Agrawal, D. (1999). Microwave sintering of metals, *Material World*, 7(11), pp. 672-673.

Araszkiewicz, M., A. Koziol, A. Lupinska and M. Lupinski (2007). Microwave drying of various shape particles suspended in an air stream, *Transp. Porous Med*, 77, pp. 173-186.

Badics, Z., B. Ionescu and Z.J. Cendes (2004). High-order adaptive time-domain solution of non-linear coupled electromagnetic-thermal problems, *IEEE Trans. Magnetics,* 40 (2), pp. 1274-1277.

Balat-Pichelin, M. and F. Duqueroie (2001). Heat transfer modeling at high temperature for the evaluation of atomic oxygen recombination energy on ceramic materials, *Intern. J. Thermal Sci*., 40, pp. 279-287.

Balbastre, J.V., E. de los Reyes, M.C. Nuno and P. Plaza (2006). Design guidelines for applicators used in the microwave heating of high losses materials. In: *Advances in Microwave and Radio Frequency Processing*, M. Willert-Porada, Ed., Springer, pp. 31-38.

Balsa-Canto, E., A.A. Alonso and J.R. Banga (2002). Restricted second order information for the solution of optimal control problems using control vector parameterization, *J. Process Control*, 12, pp.243-255.

Banga, J.R., Z. Pan and R.P. Singh (2001). A novel, efficient and reliable method for thermal process design and optimization. Part I. Theory, *J. Food Engineering*, 52, pp. 227-234.

Banga, J.R., E. Balsa-Canto, C.G. Moles and A.A. Alonso (2003). Improving food processing using modern optimization methods, *Trends in Food Sci. and Technology*, 14, pp. 131-144.

Bernhard, J.T. and W. Joines (1996). Dielectric slab-loaded resonant cavity for applications requiring enhanced field uniformity, *IEEE Trans. on Microwave Theory Tech*., 44, pp. 457-460.

Bradshaw, S., T.V. Chow Ting Chan, H.C. Reader, R. Geschke, S.A. Kingman and K. Jackson (2003), Quantifying applicator design for microwave assisted comminution, *Proc. 9th Conf. Microwave and High-Frequency Heating*, *Loughborough, U.K.*, pp. 509-512.

Bradshaw, S., S. Delport and E. van Wyk (1997). Qualitative measurement of heating uniformity in a multimode microwave cavity, *J. Microwave Power & Electromag. Energy*, 32 (2), pp. 87-95.

Brelid, P.L. and R. Simonson (1999). Acetylation of solid wood using microwave heating, *Holz als Roh- und Werkstoff*, 57, 383-389.

Buffler, C.R. (1993). *Microwave cooking and processing: Engineering fundamentals for the food scientist*, Van Nostrand Reinhold, N.Y.

Bykov, Yu.V., K.I. Rybakov and V.E. Semenov (2001). High-temperature microwave processing of materials, *J. Appl. Phys*., 34, pp. 55-75.

Celuch, M., W. Gwarek and S. Sypniewski (2006). A novel FDTD system for microwave heating and thawing analysis with automatic time-variation of enthalpy-dependent media parameters, In: *Advances in Microwave and Radio Frequency Processing*, M. Willert-Porada, Ed., Springer, pp. 199-209.

Chan, T.V.C.T. and H.C. Reader (2000). *Understanding Microwave Heating Cavities*, Artech House, Boston-London.

Choi, C.T.M. and A. Konrad (1991). Finite element modeling of RF heating process, *IEEE Trans. Magnetics,* 27 (5), pp. 4227-4230.

Clemens, J. and C. Saltiel (1996). Numerical modeling of materials processing in microwave furnaces, *Int. J. Heat Mass Transfer*, 39 (8), pp. 1665-1675.

Craven, M.P., T.E. Cross and J.G.P. Binner (1996). Enhanced computer modeling for high temperature microwave processing of ceramic materials, *Proc. MRS 5th Symp. Microwave Processing of Materials*, 430, pp. 351-356.

Datta, A.K. (2001). Fundamentals of heat and moisture transport for microwaveable food product and process development, In: *Handbook of Microwave Technology for Food Applications*, A.K. Datta and R.C. Anantheswaran, Eds., Marcel Dekker, Inc., pp. 115-172.

Domínguez-Tortajada, E., J. Moznó-Cabrera and A. Díaz-Morcillo (2005). Load matching in microwave-heating applicators by means of genetic-algorithm optimization of dielectric multilayer structures, *Microwave Opt. Tech. Letters* 47(5): 426-430.

Dominguez-Tortajada, E., J. Monzo-Cabrera and Al. Diaz-Morcillo (2007), Uniform electric field distribution in microwave heating applicators by means of genetic algorithms optimization of dielectric multilayer structures, *IEEE Trans. Microwave Theory Tech.,* 55 (1), pp. 85-91.

Egorov, S.V., A.G. Eremeev, I.V. Plotnikov, V.E. Semenov, A.A. Sorokin, N.A. Zharova and Yu.V. Bykov (2006). Edge effect in microwave heating of conductive plates, *J. Phys. D: Appl. Phys*., 39, pp. 3036-3041.

Feher, L., M. Thumm and K. Drechsler (2006). Gigahertz and nanotubes – perspectives for innovations with movel industrial microwave processing technology, *Adv. Eng. Mater*., 8(1-2), pp. 26-32.

Feldman, D., E. Kiley, S.L. Weekes and V.V. Yakovlev (2007). 1D and 2D coupled electromagnetic-thermal models for combined microwave-convective heating in a pulsing regime, *J. Microwave Power & Electromag. Energy*, 41, to be published.

Gjonaj, E., M. Bartsch, M. Clemens, S. Schupp and T. Weiland (2002). High-resolution human anatomy models for advanced electromagnetic field computations, *IEEE Trans. Magnetics,* 38 (2), pp. 357-360.

Groombridge, P., A. Oloyede and E. Siores (2000). A control system for microwave processing of materials, *J. Manufacturing Science & Engng*, 122, pp. 253-261.

Gunasekaran, S. (1990). Grain drying using continuous and pulsed microwave energy, *Drying Technology*, 8(5), pp. 1039-1047.

Gunasekaran, S. and H.-W. Yang (2007a). Effect of experimental parameters on temperature distribution during continuous and pulsed microwave heating, *J. Food Engineering*, 78, pp. 1452-1456.

Gunasekaran, S. and H.-W. Yang (2007b). Optimization of pulsed microwave heating, *J. Food Engineering*, 78, pp. 1457-1462.

Gwarek, W.K. and M. Celuch (2006). A review of microwave power applications in industry and research, *Proc. 15th Conf. on Microwaves, Radar, and Wireless Communications (MIKON-2006), Krakow, Poland,* pp. 843-848.

Gwarek, W.K. and M. Celuch (2007). Properties of the FDTD method relevant to the analysis of microwave power problems, *J. Microwave Power & Electromag. Energy*, 41, to be published.

Haugh, C., E.S. Davidson, N.A.M. Estes III and P.J. Wang (1997). Pulsing microwave energy: a method to create more uniform myocardial temperature gradients, *J. Interventional Cardiac Electrophysiology*, 1, pp. 57-65.

Heidemann, M., H. Garbe and R. Kebel (2000). Calculation of electromagnetically and thermally coupled fields in real soil decontamination, *Proc. 15th Intern. Symp. on EMC, Wroclaw*, pp. 289-293.

Hill, J.M. and T.R. Marchant (1996). Modeling microwave heating, *Appl. Math. Modeling*, 20 (1), pp. 3-15.

Huo, Y. and B.Q. Li (2005). Boundary/finite element modeling of three-dimensional electromagnetic heating during microwave food processing, *J. Heat Transfer*, 127(10), pp. 1159-1166.

Itaya, Y., S. Uchiyama and S. Mori (2007). Internal heating effect and enhancement of drying of ceramics by microwave heating with dynamic control, *Transp. Porous Med*., 66, pp. 29-42.

Jolly, P.G. (1986). Temperature controlled combined microwave-convection drying, *J. Microwave Power & Electromag. Energy*, 21 (2), pp. 65-74.

Jolly, P.G. and I. Turner (1990). Non-linear field solution of one-dimensional microwave heating, *J. Microwave Power & Electromag. Energy*, 25 (2), pp. 3-15.

Jumah, R.Y. and G.S.V. Raghavan (2001). Analysis of heat and mass transfer during combined microwave conventive souped-bed drying, *Drying Technology*, 19(3-4), pp. 485-506.

Kappe, C.O. and A. Stadler (2005). *Microwaves in Organic and Medicinal Chemistry*, Wiley-VCh.

Knoerzer, K. (2006). *Simulation von Mikrowellen-prozessen und Validierung mittels bildgenebender magnetischer Resonanz*, Ph.D. Thesis, University of Karlsruhe.

Knoerzer, K., M. Regier, H. Schubert and H.P. Schuchmann (2006). Controlled simulations of microwave thermal processing of arbitrarily shaped foods, *Proc. 40th IMPI Microwave Power Symp., Boston, MA, August 2006*, pp. 213-216.

Kolomeytsev, V.A. and V.V. Yakovlev (1993). Family of operating chambers for microwave thermal processing of dielectric materials, *Proc. 29th Microwave Power Symp., Chicago, IL, July 1993*, pp. 181-186.

Komarov, V.V. and V.V. Yakovlev (2007). CAD of efficient TM_{mn0} single-mode elliptical applicators with coaxial excitation, *J. Microwave Power & Electromag. Energy*, 40 (3), pp. 174-185.

Kopyt, P. and M. Celuch (2003a). FDTD modeling and experimental verification of electromagnetic power dissipated in domestic microwave oven, *J. Telecommunications and Information Technology*, (1), pp. 59-65.

Kopyt, P. and M. Celuch (2003b). Coupled electromagnetic and thermal simulation of microwave heating process, *Proc. 2nd Workshop on Information Technologies and Computing Techniques for the Agro-Food Sector, Barcelona, November 2003*, pp. 51-54.

Kopyt, P. and M. Celuch (2005a). Coupled simulation of microwave heating effect with *QuickWave-3D* and *Fluent* simulation tools, *Proc. 10th AMPERE Conf. Microwave and High Frequency Heating, Modena, Italy*, pp. 440-443.

Kopyt, P. and M. Celuch (2005b). Towards a multiphysics simulation system for microwave power phenomenon, *Proc. 2005 Asia-Pacific Microwave Conf., Suzhou, China*, pp. 2877-2880.

Kopyt, P. and M. Celuch (2007). Coupled electromagnetic-thermodynamical simulation of microwave heating problems using the FDTD algorithm, *J. Microwave Power & Electromag. Energy*, 41, to be published.

Lagos, L.E., W. Li, M.A. Ebadian, T.L. White, R.G. Grubb and D. Foster (1995). Heat transfer within a concrete slab with a finite microwave heating source, *Int. J. Heat Mass Transfer*, 38 (5), pp. 887-897.

Leparoux, S., S. Vaucher and O. Beffort (2003). Assessment of microwave heating for sintering of Al/SiC and for in-situ synthesis of TiC, *Adv. Eng. Mater.*, 5, pp. 449-453.

Lidström, P. and J. Tierney, Eds. (2005). *Microwave-Assisted Organic Synthesis*, Blackwell Scientific.

Loupy, A., Ed. (2006). *Microwaves in Organic Synthesis*, Wiley-VCh.

Lu, C.-C., H.Z. Li and D. Gao (2000). Combined electromagnetic and heat-conduction analysis of rapid rewarming of cryopreserved tissues, *IEEE Trans. Microwave Theory Tech.,* 48(11), pp. 2185-2190.

Lurie, K.A. and V.V. Yakovlev (1999). Method of control and optimization of microwave heating in waveguide systems, *IEEE Trans. Magnetics*, 35 (3), pp. 1777-1780.

Lurie K.A. and V.V. Yakovlev (2002), Control over electric field in traveling wave applicators, *J. Engng Math*, 44(2), pp. 107-123.

Ma, L. D.-L. Paul, N. Pothecary, C. Railton, J. Bows, L. Barratt, J. Mullin, D. Simons (1995). Experimental validation of a combined electromagnetic and thermal FDTD model of a microwave heating process, *IEEE Trans. Microwave Theory Tech.,* 43(11), pp. 2565-2572.

Mechenova, V.A. and V.V. Yakovlev (2004). Efficiency optimization for systems and components in microwave power engineering, *J. Microwave Power & Electromag. Energy*, 39 (1), pp. 15-29.

Metaxas, A.C. and R. Meredith (1983). *Industrial Microwave Heating*, Peter Peregrinus, London.

Michalski, K.A. and H.S. Jabs (2000). One-dimensional analysis of microwave batch sterilization of water with continuous impedance matching, *Microwave Opt. Tech. Letters*, 26(2), pp. 83-89.

Microwave Processing of Materials (1994), National Research Council, Publication NMAB-473, Washington, DC.

Monzó-Cabrera, J., A. Díaz-Morcillo, J.L. Pedreño-Molina and D. Sánchez-Hernández (2004). A new method for load matching in multimode-microwave heating applicators based on the use of dielectric-layer superposition, *Microwave Opt. Tech. Letters* 40(4), pp. 318-322.

Monzó-Cabrera, J., A. Diaz-Morcillo and E. Domínguez-Tortajada (2007). Genetic algorithm optimization of dielectric casts for uniform electric field pattern synthesis, *Proc. 9th Seminar Computer Modeling & Microwave Power Engineering, Valencia, Spain*, pp. 6-7.

Murphy, E.K. and V.V. Yakovlev (2006). RBF network optimization of complex microwave systems represented by small FDTD modeling data sets, *IEEE Trans. on Microwave Theory Tech*. 54(7), pp. 3069-3083.

Nott, K.P., L.D. Hall, J.R. Bows, M. Hale and M.L. Patrick (1999). Three-dimensional MRI mapping of microwave induced heating patterns*, Intern. J. Food Science and Technology*, 34, pp. 305-315.

Ohlsson, T., B. Wappling-Raaholt, L. Ahrne, U.-K. Barr (2006). Microwave research for the food industry – some recent and future applications, *Proc. 10th AMPERE Conf. Microwave and RF Heating, Modena, Italy, Sept. 2006*, pp. 285-289.

Pedreño-Molina, J.L., J. Monzó-Cabrera and J.M. Catalá-Civera (2007). Sample movement optimization for uniform heating in microwave heating ovens, *Int. J. RF & Microwave CAE*, 17 (2), pp. 142- 152.

Petzoldt, F., B. Scholz, H.S. Park and M. Willert-Porada (2006). Microwave sintering of PM steels, In: *Advances in Microwave and Radio Frequency Processing*, M. Willert-Porada, Ed., Springer, pp. 598-608.

Pichon, L. and O. Meyer (2002). Coupled thermal-electromagnetic simulation of a microwave curing cell, *IEEE Trans. Magnetics,* 38 (2), pp. 977-980.

Pitarch, J., A.J. Canós, F.L. Peñaranda-Foix, J.M. Catalá-Civera and J.V. Balbastre (2003). Synthesis of uniform electric field distributions in microwave multimode applicators by multifeed techniques, *Proc. 9th Conf. Microwave and High-Frequency Heating*, *Loughborough, U.K.*, pp. 221–224.

Plaza-Gonzalez, P., J. Monzó-Cabrera, J.M. Catalá-Civera, and D. Sánchez-Hernández (2004). New approach for the prediction of the electric field distribution in multimode microwave-heating applicators with mode stirrers, *IEEE Trans. Magn.*, 40 (3), pp. 1672–1678.

Plaza-Gonzalez, P., J. Monzó-Cabrera, J.M. Catalá-Civera and D. Sánchez-Hernández (2005). Effect of mode-stirrer configurations on dielectric heating performance in multimode microwave applicators, *IEEE Trans. Microwave Theory Tech.* 53 (5), pp. 1699–1706.

Rabello, A.A., E.J. Silva, R.R. Saldanha, C. Vollaire and A. Nicolas (2005). Adaptive time-stepping analysis of non-linear microwave heating problem, *IEEE Trans. Magnetics,* 41 (5), pp. 1584-1587.

Ratanadecho, R., K. Aoki and M. Akahori (2002a). The characteristics of microwave melting of frozen packed beds using a rectangular waveguide, *IEEE Trans. Microwave Theory Tech.,* 50 (6), pp. 1495-1502.

Ratanadecho, R., K. Aoki and M. Akahori (2002b). A numerical and experimental investigation of the modeling of microwave heating for liquid layers using a rectangular wave guies (effects of natural convection and dielectric properties), *Applied Math. Modeling,* 26, pp. 449-472.

Requena-Pérez, M.E., J.L. Pedreño-Molina, M. Pinzolas-Prado, J. Monzó-Cabrera, A. Díaz-Morcillo and D. Sánchez-Hernández (2004). Load matching in multimode microwave-heating applicators by load location optimization, *Proc. 34th European Microwave Conf., Amsterdam, 2004*, pp. 1549-1552.

Risman, P.O. and M. Celuch (2000). Electromagnetic modeling for microwave heating applications, *Proc. 13th Conf. on Microwaves, Radar, and Wireless Communications (MIKON-2000), Wroclaw, Poland,* pp. 167-182.

Roussy, G. and J. Pearce (1995). *Foundations and industrial applications of microwaves and radio frequency fields*, Wiley, N.Y.

Sabliov, C.M., K.P. Sandeep and J. Simunovic (2005). High frequency electromagnetism coupled with conductive heat transfer – a method to predict temperature profiles in materials heated in a focused microwave oven, Microwave and Radio Frequency Applications, *Proc. 4th World Congress on Microwave and Radio Frequency Applications, November, 2004, Austin, TX*, pp. 469-476.

Sabliov, C.M., D.A. Salvi and D. Boldor, High frequency electromagnetism, heat transfer, and fluid flow coupling in ANSYS *Multiphysics* to numerically solve for temperature of a liquid product heated in a continuous flow focused microwave system, *J. Microwave Power & Electromag. Energy*, 41, to be published.

Salagnac, P., P. Glouannec and D. Lecharpentier (2004). Numerical modeling of heat and mass transfer in porous medium during combined hot air, infrared and microwave drying, *Intern. J. Heat and Mass Transfer*, 47, pp. 4479-4489.

Schaefer, M.D. (1999). *Microwave Tempering of Shrimp with Susceptors*, M.S. Thesis, Virginia Polytechnic Institute and State University.

Sekkak, A., L. Pichon and A. Razek (1994). 3-D FEM magneto-thermal analysis in microwave oven, *IEEE Trans. Magnetics,* 30 (5), pp. 3347-3350.

Sundberg, M., P.-S. Kildal and T. Ohlsson (1998). Moment method analysis of a microwave tunnel oven, *J. Microwave Power & Electromag. Energy*, 33 (1), pp. 36-48.

Swanson, D.G. and W.J.R. Hoefer (2003). *Microwave Circuit Modeling Using Electromagnetic Field Simulation*, Artech House, Boston-London.

Tilford, T., E. Baginski, J. Kelder, A.K. Parrott and K.A. Pericleous (2007). Microwave modeling and validation in food thawing applications, *J. Microwave Power & Electromag. Energy*, 41, to be published

To, E.C., R.E. Mudgett, D.I.C. Wang. S.A. Goldblith and R.V. Decareau (1974). Dielectric properties of food materials, *J. Microwave Power*, 9 (4), pp. 303-315.

Torres, F. and B. Jecko (1997). Complete FDTD analysis of microwave heating processes in frequency-dependent and temperature-dependent media, *IEEE Trans. Microwave Theory Tech.,* 45 (1), pp. 108-117.

Thuery, J. (1992). Microwaves: Industrial, Scientific and Medical Applications, Artech House, Boston-London.

Wappling-Raaholt, B., P.O. Risman and T. Ohlsson (2006). Microwave heating of ready meals – FDTD simulation tools for improving the heating uniformity, In: *Advances in Microwave and Radio Frequency Processing*, M. Willert-Porada, Ed., Springer, pp. 243-255.

Wäppling-Raaholt, B. and T. Ohlsson (2006). Improving the heating uniformity in microwave processing, In: The Microwave Processing of Foods, H. Schubert and M. Regier, Eds., CRC, pp. 292-316.

Whittaker, A.G. and D.M.P. Mingus (1994). The application of microwave heating to chemical synthesis, *J. Microwave Power & Electromagnetic Energy*, 29(4), pp. 195-220.

Yakovlev, V.V. (2001), Commercial EM codes suitable for modeling of microwave heating - a comparative review, In: *Scientific Computing in Electrical Engineering*, *Lecture Notes in Computational Sciences and Engineering*, U. van Reinen, M. Gunther, D. Hecht, Eds., 18, Springer, pp. 87-96, 2001.

Yakovlev, V.V. (2006), Examination of contemporary electromagnetic software capable of modeling problems of microwave heating, In: *Advances in Microwave and Radio Frequency Processing*, M. Willert-Porada, Ed., Springer, pp. 31-38.

Yang, H.-W. and S. Gunasekaran (2001). Temperature profiles in a cylindrical model food during pulsed microwave heating, *J. Food Scie*nce, 66(7), pp. 998-1004.

Yang, H.-W. and S. Gunasekaran (2004). Comparison of temperature distribution in model food cylinders based on Maxwell's equations and Lambert's law during pulsed microwave heating, *J. Food Engineering*, 64, pp. 445-453.

Yongsawatdigul, J. and S. Gunasekaran (1996). Microwave-vacuum drying of cranberries: Part 1. Energy use and efficiency, *J. Food Processing & Preservation*, 20, pp. 121-143.

Zhang, H and A. Datta (1999). Coupled electromagnetic and thermal modeling of microwave oven heating of foods, *J. Microwave Power & Electromag. Energy*, 35 (2), pp. 71-76.

Zhang, H. and A.K. Datta (2000). Electromagnetics of microwave heating: magnitude and uniformity of energy absorption in an oven, In: In: *Handbook of Microwave Technology for Food Applications*, A.K. Datta and R.C. Anantheswaran, Eds., Marcel Dekker, Inc., pp. 33-67.

Zhao, H. and I.W. Turner (2000). The use of coupled computational model for studying the microwave heating of wood, *Applied Math. Modeling,* 24, pp. 183-197.

Zhu, J., A.V. Kuznetsov and K.P. Sandeep (2007). Mathematical modeling of continuous flow microwave heating of liquids (effects of dielectric properties and design parameters), *Intern. J. Thermal Sciences*, 46, pp. 328-341.